HHS Public Access

Author manuscript

Front Biosci (Landmark Ed). Author manuscript; available in PMC 2015 March 19.

Published in final edited form as:

Front Biosci (Landmark Ed). ; 20: 515–555.

Cilia/Ift protein and motor-related bone diseases and mouse models

Xue Yuan[1] and **Shuying Yang**[1,2]

[1]Department of Oral Biology, School of Dental Medicine, University at Buffalo, The State University of New York, 3435 Main Street, Buffalo, NY, 14214, USA

[2]Developmental Genomics Group, New York State Center of Excellence in Bioinformatics and Life Sciences, University at Buffalo, The State University of New York, 701 Ellicott St, Buffalo, NY, 14203, USA

Abstract

Primary cilia are essential cellular organelles projecting from the cell surface to sense and transduce developmental signaling. They are tiny but have complicated structures containing microtubule (MT)-based internal structures (the axoneme) and mother centriole formed basal body. Intraflagellar transport (Ift) operated by Ift proteins and motors are indispensable for cilia formation and function. Mutations in Ift proteins or Ift motors cause various human diseases, some of which have severe bone defects. Over the last few decades, major advances have occurred in understanding the roles of these proteins and cilia in bone development and remodeling by examining cilia/Ift protein-related human diseases and establishing mouse transgenic models. In this review, we describe current advances in the understanding of the cilia/Ift structure and function. We further summarize cilia/Ift-related human diseases and current mouse models with an emphasis on bone-related phenotypes, cilia morphology, and signaling pathways.

Keywords

Ift proteins; Ift motors; Ciliopathies; Mouse models; bone; ENU; Gene trap; Knockout; Review

2. INTRODUCTION

Normal vertebrate skeletons, composed of cartilage and bone, are critical for locomotion, respiration, and protection of the vital organs (1). Both cartilage and bone are derived from embryonic mesenchyme (2, 3). Hyaline cartilage is the most widespread cartilage and prevails in the fetal skeleton, while bone is predominant at a later stage and persists postnatally throughout life (1). Most bones are formed by replacement of existing cartilage rudiments. This process is known as endochondral bone formation, which starts with embryonic mesenchymal cells condensing at the sites where the skeletal elements will form. The condensed mesenchymal cells result in the formation of the cartilaginous anlagen, which later is ossified to become bone by osteoblasts (4–6). In contrast, mesenchymal

Send correspondence to: Dr. Shuying Yang, Department of Oral Biology, School of Dental Medicine, University at Buffalo, The State University of New York, B36 Foster Hall, Buffalo, NY 14214. Tel: 716-829-6338, Fax: 716-829-3942, sy47@buffalo.edu.

condensations that prefigure the clavicles, mandible, and certain bones of the skull, directly differentiate into osteoblasts. This process does not require a cartilaginous template and is called intramembranous ossification (1–3). Skeletal formation and homeostasis are strictly controlled by systemic and local regulators, such as Wnt, Hedgehog (Hh) (7), Notch (8), bone morphogenetic protein 2 (BMP2) (9), and thyroid hormones (10, 11). It has uncovered over 300 genetic diseases with disorders in the growth and development of the skeleton (12). Bone development abnormalities often lead to bony deformities that severely impact patients' quality of life and general health and sometimes lead to premature death (1, 2, 13, 14). Among these genetic diseases, a certain groups are caused by disorders of the primary cilia (15).

Primary cilia are small microtubule (MT) based organs that are projected from the surface of nearly every mammalian cells and function as antennae. They sense a diverse range of extracellular signals, such as growth factors and hormones, through various surface receptors localized on the ciliary membrane, and transmit the signals back into the nucleus. Thus cilia are important for embryonic and postnatal development of many vital organs (16–18). Defects of cilia or cilia-related protein cause a wide variety of human disease symptoms, including polycystic kidneys, hydrocephalus, vision and hearing loss as well as severe bone abnormalities, suggesting that the role of cilia in multiple organ development is indispensable (18–25).

Intraflagellar transport (Ift), a bidirectional transport system run by Ift protein complexes and Ift motors, is found to be essential for building cilia and maintaining cilia function (26, 27). Ift protein complexes are formed with complex A and complex B containing about 20 Ift proteins (28). Mutations in Ift proteins (such as Ift80, Ift122, and Ift43) or Ift motors (such as DYNC2H1) usually lead to cilia defects and human diseases (29–31). Those groups of human diseases with primary cilia malfunction display disorders of multiple organs, including kidney, liver, brain, and limb (30) and are called ciliopathies (29, 32). A certain portion of ciliopathies, such as Jeune asphyxiating thoracic dystrophy (JATD) and short rib polydactyly syndromes (SRP), result in several bone defects, suggesting the important role of cilia in bone development (29, 33–35).

During the 1960s, scientists found cilia present in chondrocytes (36). Subsequent work has revealed that cilia are also present in osteoblasts, osteocytes, and mesenchymal stem cells (37–41). Bone is a sensitive and dynamic tissue that constantly remodels to meet the demands of its environment (42, 43). Cilia are considered to function as chemosensors and mechanosensors for bone formation and maintenance (43–45). Multiple bone developmental signaling pathways, such as Hh and Wnt signaling pathways, have been linked to primary cilia, Ift proteins and motors (46–49). Both Indian hedgehog (Ihh) and Sonic hedgehog (Shh) are required for skeletal development (50–53). Ihh is an important signaling molecule in endochondral ossification because Ihh null mice display shortened face and tail with extremely short limbs and narrow rib cages (51). Shh is required for the early stage of patterning of the limb (54, 55). Genetic screens for embryonic patterning mutations first uncovered the connection between mammalian Hh signaling and primary cilia (56). Since then, the Hh pathway has become the most intensively studied pathway among the cilia-related signaling pathways (see review (57) and (58)). It is now clearly established that the

core components of Hh signaling pathway, including Hh receptor Patched 1 (Ptch1), Smoothened (Smo) protein, and Gli transcription factors are localized to cilia (57). Ptch1 is found at the base of primary cilia in the absence of Hh. Upon exposure to Hh, Ptch1 moves out of cilia (59, 60), and then Smo moves into the cilia and shifts the Gli process from a transcriptional repressor to transcriptional activator (61). Functional intact cilia are required for the Hh signaling transduction, and mutations in cilia/Ift proteins and motors disrupt Hh signaling pathway. However, mutations in different genes lead to different phenotypes, suggesting the distinct roles of individual Ift proteins and motors in Hh signaling or their involvement of other signaling pathways (57). Wnt pathway is another critical pathway for skeletal development and homeostasis (62, 63). However, the relationship between Wnt and primary cilia is controversial (58, 64). Wnt signaling cascades can be broadly divided into two general categories: 1) canonical Wnt/β-catenin pathway (stabilizing the transcription of co-activator β-catenin and therefore turning on gene expression) and 2) the non-canonical Wnt/planar cell polarity (PCP) pathway (65). Different mutations in cilia/Ift proteins cause different changes in Wnt signaling pathway (64, 66, 67). However, the role of cilia/Ift proteins and motors in Wnt signaling transduction remains largely unknown.

To study the fundamental biology of cilia/Ift proteins and motors, various animal models, including tetrahymena thermophila, zebrafish, and mouse, have been developed (68–70). Mouse is genetically and pathophysiologically similar to human and relatively easy to be genetically manipulated. Therefore, mouse has become the favorite and reliable mammalian model for studies of bone biology (71, 72). Within the last decade, significant progress in the understanding of the cilia/Ift proteins and motors in bone development and diseases has been made using various mouse genetic models and we summarize those advances here.

3. STRUCTURE OF IFT PROTEINS/MOTORS AND CILIA

The structure of the cilia is conserved throughout evolution. When cell is in G_0 stage, primary cilium is generated from a “mother” centriole of the centrosome, which becomes the basal body in the cilia structure (73). Centriole is a cylinder comprising nine triplet MTs that provide the template for the formation of an MT-based internal structure (the axoneme) (74). Two of the most common axoneme architectures are “9 + 2” for motile cilia (9 peripheral MT doublets and 2 single central MTs) and “9 + 0” for primary cilia (only 9 peripheral MT doublets) (75). Since ribosome and membrane vesicles are absent from the cilia, ciliary proteins have to be synthesized in the cytoplasm and actively transported into the cilia along MTs (73). This highly conserved process is called Ift (76), which moves macromolecules from the base to the tip of a cilium (anterograde transport) and from the tip of the cilium back to the cell body (retrograde transport) (77). Effective Ift involves the Ift complexes and Ift motors. It is believed that the heterotrimeric kinesin-II motor protein drives the anterograde transport (78), whereas cytoplasmic dynein-2 moves the rafts back in the retrograde direction (79).

Ift complexes serve as adaptors to mediate the contacts between cargo proteins and motors (80). Ift was first reported in *Chlamydomonas* in 1993 by Kozminski *et al* (76, 81), and later Ift particles were identified in *Chlamydomonas* by biochemical purifications (82, 83). By biochemical purification, Cole *et al* first reported that Ift complex has two sub-complexes

named complex A (Ift-A) and complex B (Ift-B) (82). Subsequently, four proteins in complex A (Ift144, Ift140, Ift139 and Ift122) and eleven proteins in complex B (Ift172, Ift88, Ift81, Ift80, Ift74, Ift72, Ift57/55, Ift52, Ift46, Ift27 and Ift20) have been identified (82). The proteins were named according to their size (in kD). Later, Ift43 and then Ift121 were identified in the complex A (82, 84, 85). Thus complex A is thought to be composed of six subunits including Ift144, Ift140, Ift139, Ift122, Ift43 and Ift121.

Ift-B complex is more complicated and contains 14 known proteins (Ift20, Ift22, Ift25, Ift27, Ift46, Ift52, Ift54, Ift57, Ift70, Ift74/Ift72, Ift80, Ift81, Ift88 and Ift172) (18, 82, 85, 86). Lucker *et al* used increased ionic strength to dissociate the Ift-B of *Chlamydomonas reinhardtii* and found that the biochemically intact core of Ift-B contains Ift88, Ift81, Ift74/72, Ift52, Ift46, and Ift27 (87). Ift72 and Ift74 are derived from the same gene and present in a 1:1 stoichiometry. So it is usually combined into a single term, Ift74/72 (87, 88). The other subunits including Ift172, Ift80, Ift57, and Ift20 are not required for the core and can be disassociated with the core by using a high salt concentration. Among those core proteins, Ift81 and Ift74/72 are believed to form a tetrameric complex to serve as a scaffold for the interaction with other subunits (87).

All of the Ift proteins are conserved in mammals. Ift proteins are typically found along the cilia and in the base of the cilia (89). Anterograde transport is regulated by Ift-B, while the retrograde transport is related to Ift-A (28, 90). Mutations in Ift-B usually block cilia assembly (91, 92), similar to kinesin-II mutation (93, 94), while defects in Ift-A protein(s) typically result in malformed cilia with accumulation and function defects of Ift proteins (95–97) that resemble the mutations in cytoplasmic dynein-2 (48) (Figure 1).

Besides Ift motors and Ift complexes, sixteen identified Bardet–Biedl syndrome proteins (BBS1-16) are also important for cilia formation and maintenance. Seven highly conserved BBS proteins (BBS1, BBS2, BBS4, BBS5, BBS7, BBS8 and BBS9) and one newly defined interacting protein BBIP10 formed BBSome (98, 99). BBSome is indispensable for ciliary membrane biogenesis, microtubule stability, and acetylation (99). Other BBS proteins have a variety of functions including guanosine triphosphate hydrolases (GTPase) and ubiquitin ligase (See review (100)).

A large amount of cargo proteins have been found in the cilia or associated with cilia structures (75). Those proteins include the signaling components such as Gli and Smo in the Hh signaling pathway. Some of them are proteins located at a specific region of the cilium to regulate cilia formation or cilia-related signaling transduction such as Ellis-van Creveld syndrome protein homolog (Evc) and oral-facial-digital syndrome 1 (OFD1) (101, 102). Mutations of those proteins also cause ciliopathies.

4. CILIA/IFT PROTEIN AND MOTOR-RELATED HUMAN DISEASES

Cilia were first found in the kidneys and the thyroid gland one century ago (103). Subsequently, cilia have been found in many other organs and cell types (31). Further work revealed a dozen human genetic diseases caused by cilia-related gene mutation, which are commonly called as ciliopathies (31, 104). Those disorders includes BBS, OFD, Meckel-Gruber syndrome (MKS), Joubert syndrome (JBTS)/JBTS-related disorder (JSRD), JATD,

Leber congenital amaurosis (LCA), Primary ciliary dyskinesia (PCD)/Kartagener syndrome (KS), Ellis-van Creveld syndrome (EVC), Nephronophthisis (NPHP), Senior-Loken syndrome (SLS), autosomal dominant and recessive polycystic kidney disease (ADPKD and ARPKD), Usher syndrome (US), and Alström syndrome (ALMS) (104, 105). Those ciliopathies share common clinical features and involve many major organs, including kidney, brain, limb, retina, liver, and bone (29, 32, 104, 105).

More than 30 different genes have been linked to the skeletal-related ciliopathies. These are dynein-2 motor (*Dync2h1*), Ift genes (*Ift80, Ift122, Ift43, Ift140, WDR35, WDR19,* and *TTC21B*) as well as the genes responsible for the basal body (*NEK1, Evc, Evc2, BBS1-16, OFD1, MKS1, MKS3, TMEM216, CEP290, RPGRIP1L, CC2D2A, TCTN2, B9D1, B9D2, and NPHP3*). Mutations of those genes result in common skeleton defects, including polydactyly, shortened bones, and craniofacial dysmorphology (Table 1) (29). Here, we only summarize the ciliopathies with bone phenotypes and their underlying genetic defects.

4.1. JATD and Mainzer-Saldino-Syndrome (MSS)

JATD, also known as asphyxiating thoracic dystrophy (ATD) was first reported in 1955 by Jeune *et al*. The patient with JATD had a narrow thoracic cavity and multiple cartilage anomalies, and died due to respiratory insufficiency during the early neonatal period (106). JATD is a rare autosomal recessive skeletal dysplasia with short limbs, narrow thorax, trident acetabular roof, and occasional polydactyly (107). Studies have suggested that mutations of *Ift80, DYNC2H1, TTC21B* (encoding Ift139) and *WDR19* (encoding Ift144) are associated with JATD (33, 35, 40, 108–110). Respiratory failure is the usual cause of death in JATD in early infancy (110). MSS is related to JATD but has a milder rib phenotype and additional renal and eye defects (111).

Very recently, *Ift140* mutation was identified in JATD and MSS (111, 112). It has been found that Ift140 patients display mild chest narrowing, end-stage renal failure, and ocular dysfunction (112). Ciliary abundance and localization of IFT-A proteins are changed in the fibroblasts from *Ift40* mutant patients (111).

4.2. BBS

BS is a pleiotropic genetic disorder with the phenotypes of retinal dystrophy, obesity, post-axial polydactyly, renal dysfunction, learning difficulties and hypogonadism (113). Polydactyly, hepatic fibrosis, and kidney, genital and heart malformations can be observed at birth (114). Sixteen BBS gene (*BBS1* to *BBS16*) mutations are account for 80% of BBS. The majority of mutations occur in *BBS1* and *BBS10* (114).

4.3. EVC and Weyers acrofacial dysostosis (WAD)

EVC was first reported by Richard Ellis and Simon van Creveld in 1940. Patients had retarded growth, narrow rib cage, supernumerary fingers and toes, orofacial abnormalities and heart abnormalities (115, 116). WAD was named after Helmut Weyers, who reported it in 1952. EVC and WAD are allelic disorders, but WAD has less severe symptoms and a different pattern of inheritance (117). They are both caused by the loss-of-function mutations of *Evc* or *Evc2* genes (117–121). Valencia *et al* further domonstrated that Hh

signal transduction is impaired when a mutant murine *Evc2* Weyer variant is expressed in NIH 3T3 cells (121).

4.4. OFD

OFD is an X-linked dominant inheritance disorders with 13 different described types (type I to type XIII) classified by their patterns of signs and symptoms (122, 123). The phenotype includes oral, facial, and digital anomalies (124, 125). OFD type I, which is also known as Papillon-Leage and Psaume syndrome, has the higheset incidence (122). Ferrante *et al* indentified the responsible gene *OFD1* (formerly named *Cxorf5/71–7a*) for this syndrome in 2001 (126). *OFD1* is found missense, nonsense, splice, and frameshift mutation in OFD1 patients (126). Further studies showed OFD1 is a centrosomal protein and localized in the basal body of primary cilia (102, 127). Whether *OFD1* mutation is responsible for other types of OFD is not clear now.

4.5. SRP

SRP is a group of lethal skeletal dysplasia that are characterized by short limbs, narrow thorax, polydactyly, and multiple anomalies of major organs (128). Four lethal types have been described based on radiological findings, including Saldino-Noonan syndrome (type I), Majewski syndrome (type II), Verma-Naumoff syndrome (type III) and Beemer-Langer syndrome (Type IV) (34, 128). In addition, JATD and EVC are phenotypically related to SRP but are compatible with life. Recently, Ho *et al* suggested that JATD and SRP type III are variants of the same disorder and SRP type III has more severe phentype in bone and other organs (129). Mutation of *Ift80* or *DYNC2H1* causes those diseases (35, 70, 130). Most recently, mutation of either *DYNC2H1* or *Never-in-mitosis Kinase 1* (*NEK1*), which regulates cell cycle–associated ciliogenesis, was identified in SRP type II (128, 131). A severe form of SRP was reported with in-frame homozygous deletion of exon 5 in *WDR35* (orthologous of *Ift121* in mammals) (34).

4.6. Cranioectodermal dysplasia (CED, or sensenbrenner syndrome)

CED is a rare autosomal recessive skeletal dysplasia (132). The syndromes of CED patients are similar to JATD patients as they have short stature, limbs and ribs, narrow chest, brachydactyly, renal failure, and hepatic fibrosis (132). They also show dolichocephaly with frontal bossing and craniosynostosis (133, 134). CED is genetically heterogeneous and is caused by mutations in *Ift122* (132), *Ift43* (135), *WDR35* (136, 137) or *WDR19* (109).

4.7. Meckel syndrome (MKS, or Meckel–Gruber Syndrome, Gruber Syndrome, Dysencephalia Splanchnocystica)

MKS is a severe fetal developmental disorder characterized by occipital encephalocele, cystic kidney dysplasia, fibrotic changes of the liver and polydactyly (138). MKS is genetically heterogeneous and at least ten genes have been associated with MKS, including *MKS1(Meckel syndrome, type 1)/BBS13* (encoding MKS1, localized at the ciliary body), *MKS3/TMEM67* (*Transmembrane protein 67*, encoding MECKELIN, which localized to the cilium base), *TMEM216* (encoding TMEM216, which localized to the base of the primary cilia), *CEP290/BBS14* (encoding centrosomal protein CEP290/nephrocystin-6, which is

involved in chromosome segregation and localized around the centrosome), *RPGRIP1L* (encoding RPGRIP1L, which colocalizes to the basal body and centrosomes), *CC2D2A* (encoding CC2D2A, which localizes to basal body and the transition zone), *TCTN2* (encoding TCTN2, which localizes to transition zone), *B9D1* (encoding B9D1, which localizes to the transition zone complex), *B9D2* (encoding B9D2, which localizes to the transition zone complex), and *NPHP3* (nephrocystin-3, encoding NPHP3, which localizes to the primary cilia) (139–144).

Karmous-Benailly discovered mutations in *BBS2*, *BBS4*, and *BBS6* in MSK patients. They suggested that prenatal presentation of BBS may mimic MKS (114).

5. FUNCTION OF IFT PROTEINS OR MOTORS IN EXISTING MOUSE MODELS

To deeply understand the function of cilia-related proteins, a variety of mouse genetic models have been generated in which Ift proteins or motors are inactivated by using different genetic mutant approaches. To make the summary of Ift proteins and motors clearly understood, we first briefly introduce the most commonly used techniques to generate gene mutation models in mice as described in section 5.1., and then further summarize the published mouse models that have mutations in Ift proteins and motors. We focus on the bone-related phenotypes, ciliogenesis, and altered signaling pathways.

5.1. Methods to generate gene mutational mouse models

There are two main methods to generate gene mutational mouse models. One is directed and disease driven; and the other is non-directed, randomly generated mutation. The common directed techniques include most powerful method of transgenesis. The non-directed, random mutation-driven method is the application of radiation and chemicals such as N-ethyl-N-nitrosourea (ENU) to induce mutations (145).

Transgenesis can be accomplished by two methods. One is pronuclear injection of fertilized oocytes, which is predominantly used to overexpress endogenous or mutant proteins. The other approach is using homologous recombination to modify embryonic stem cells (ESCs). The modified ESCs are then injected into mouse blastocysts to create mutant mice (knockout mice) (146, 147). Knockout mouse models can be divided into two categories: conventional and conditional knockout. In the conventional knockout model, the target gene is permanent inactivation in all cells of the body. However, this usually causes prenatal death, which makes identification of phenotype difficult. The development of the Cre-LoxP recombination system for conditional gene knockout limits the deletion of a target gene to the desired tissue and has dramatically improved knockout mouse studies (148, 149). Osteoblast-, osteoclast-, chondrocyte-, and osteocyte-specific Cre expression has been created with various promoters to turn on the Cre expression at various differentiation stages and in different cell lineages (See reviews (150) and (72)). Although transgenic mouse models provide a powerful approach to study gene function, the Cre-LoxP recombination system is not perfect. The generation of these models is time and money consuming.

Moreover, Cre expression leaking to other cell types and the toxicity of high Cre levels are still the issues that need to be resolved (148, 149, 151).

ENU-induced mutation is one of those approaches that allow genome-wide, high-throughput research (146). ENU is the most potent germ line mutation inducer in rodents (152). ENU treatment of male mice results in random point mutations in the main targets of ENU in the spermatogonial stem cells. By breeding these male mice with normal female mice, the generated F1 population carries unique random ENU-induced mutations. Both genotype-driven and phenotype-driven approaches can be used for screening (146). In addition, the point mutation introduced by ENU resembles the most common form of human genetic variation (146), which makes it a powerful tool to study the specific genes. Large ENU screens have already yielded several mutations in Ift-related genes showing skeletal abnormalities.

Gene trapping is another technique that randomly generates loss-of-function mutations, which takes the middle path between random (such as ENU induced) and molecularly defined mutations (such as knockout mutation) (153). Gene trapping is performed with gene-trap vectors, which usually contain a promoterless reporter and/or selectable marker gene and a downstream polyadenylation sequence. When an expressed gene is inserted into the gene-trap vector, the reporter/selectable marker gene is expressed with the upstream exons, but the gene is prematurely terminated due to the inserted polyadenylation sequence (153, 154). In this way, the gene inactivation and transcriptional activity report can be achieved at the same time. The libraries of ESC lines containing mutations in single genes have been created and about 70 percent of protein-coding genes in the mouse genome have been inactivated in this way (154).

5.2. Mouse models of Ift complex A proteins

Currently, there are six known Ift-A proteins, which are Ift139, Ift144, Ift122, WDR35, Ift143 and Ift140. The *in vitro* and *in vivo* studies of these proteins are described in the following sections (Table 2).

5.2.1. Ift139—Ift139, also termed THM1 (Tetratricopeptide Repeat Containing Hedgehog Modulator 1), is a newly identified ciliary protein (96). The gene encoding this protein is named *TTC21B* (*tetratricopeptide repeat domain 21B*), or *Thm 1*(*tetratricopeptide repeat-containing hedgehog modulator-1*) (96). Ift139 contains 1,317 amino acids (about 150 kDa) and is predicted to contain 11 tetricopeptide repeat (TPR) domains (96). Davis *et al* reported that the *TTC21B* mutation in humans causes JATD and isolated NPHP. By performing *in vitro* and *in vivo* complementation assays, they further found there is a significant enrichment of pathogenic alleles in ciliapathy cases, suggesting that *TTC21B* mutation accounts for 5% of ciliopathies cases (108).

Ift139 is highly expressed in the maxillary prominence, branchialarches, limb buds, somites, and spinal cord at embryonic day 10.5. (E10.5). A null mutant of *TTC21B/Ift139* named alien (aln) ($Ift139^{alien}$) in A/J mice by ENU mutagenesis (95, 96) results in embryonic defects in limbs, eyes, skull, and brain development (95), which are correlated with its expression pattern. *In vivo* and *in vitro* studies showed that Ift139 accumulates in cilia and

colocalizes with acetylated α-tubulin, which is similar to other Ift proteins such as Ift88 (96). Cilia in the Ift139^{alien} limb cells display short and bulb-like structures in the distal tips. Interestingly, Ift88 largely accumulates at this bulb-like structure while undetectable at the proximal ends (96). However, Smo and full-length Gli proteins (key factors of Hh pathway) still can be transported into cilia. Those data suggest that mutation of Ift139 only impairs retrograde Ift, which leads the accumulation of complex B proteins in the cilia tip and forms the bulb-like structure (96).

Further studies show that Shh pathway was inappropriately activated in Ift139^{alien} and that overall phenotype of Ift139^{alien} was very similar to *Rab23* (a negative modulator of Shh signaling) mutants (96). The phenotype of Smo null mice was partially rescued by Ift139 deletion. Additionally, Gli2 was overactive in *Ift139* mutant, and the double mutant of *Gli2* and *Ift139* resembled the phenotype of *Gli2* mutant. Those studies suggested that Ift139 is a negative regulator in Shh pathway downstream of Smo and upstream of Gli2 (96). Consistence to this study, Stottmann *et al* reported that Shh signaling was up-regulated in the rostral portion of the Ift139^{alien} embryo, and the reduction of Shh ligand level (heterozygous for a null allele of Shh) partially rescued the phenotype (95). Besides, the levels of the β-catenin protein were not significantly altered in the mutant mice (95).

5.2.2. Ift122—Ift122 has a molecular weight of approximately 140 KD and contains seven WD40 domains at the N-terminus (132, 155). The missense mutation of *Ift122* is found in CED patients, and the fibroblasts from CED patients had significantly reduced both the numbers of primary cilia in and their length (132). Currently, two Ift122 mutant mouse models have been generated (97, 156). One mouse model named Ift122-null was generated by deletion of exon 1–3 of DNA repair gene-mediator of RNA polymerase II transcription subunit 1 (Med1). Due to the genomic overlap of *Ift122* and *Med1*, mutation in Ift122-null abrogates the expression of both *Med1* and *Ift122*. (97, 157). Ift122-null embryos had defects as early as E9.5 and died from E10.5 to E13.5 due to heart defect and diffuse hemorrhagic lesions. Other phenotypes expressed by these mice included exencephaly, rostral neural tube defect, delay in limb development, defects in the ventral portion of the head with altered development of the eyes and branchial arches. Cilia loss was found in the homozygous mutant and malformed cilia were observed in heterozygous embryos, which associated with defects in left–right asymmetry. Additionally, mutation of Ift22 reduced Gli2/Gli3 and Gli3 repressor functions, suggesting that Shh signaling is impaired (97).

Another mouse model Ift122^{sopb} was generated with ENU mutagenesis and named *sister of open brain* (*sopb*) due to the similar phenotype to *Rab23*/open brain mutants (158). *Sopb* is a null allele of *Ift122* with a T-to-C transition mutation in the start codon of *Ift122*. Ift122^{sopb} embryos died around E13.5, displayed neural defects, pre-axial polydactyly, enlarged bronchial arches, and ocular defects. Cilia frequency was normal in the neural tube of Ift122^{sopb} mice but reduced in Ift122^{sopb} MEFs. Cilia in Ift122^{sopb} were shorter but swollen along their lengths and tips, which accumulated with complex B proteins as stained with Ift88 and Ift57. The complex A protein Ift140 was undetectable in the cilia of Ift122^{sopb} cells, suggesting a role of Ift122 in facilitating complex A stability and retrograde Ift (158). Suppressor of Fused (SUFU) and Smo transportation to cilia were not affected while Gli2 and Gli3 accumulated in the cilia tips after disruption of Ift122. Ciliary localization of

TULP3, a repressor of Shh pathways, was also blocked in Ift122^{sopb}. These data suggested that Ift122 negatively regulates the Shh pathway downstream of Smo through differentially controlling the ciliary localization of the Hh pathway regulators (158). The different phenotypes observed in those two models may be caused by different mouse strain backgrounds (Ift122^{sopb} of C3Heb/FeJ and Ift122-null of C57BL/6, respectively) and/or by the effect of MED1 deletion in Ift122-null mutant (158).

5.2.3. Ift144—Ift144, coded by the gene *WDR19* (*WD repeat domain 19*), has WD40 regions and TPR protein–protein interaction domains (159). Ift144 localizes at the base and tip of the cilium in a punctate pattern along the axoneme in the mouse embryo fibroblasts (MEFs) (160). Mutation of *Ift144* causes CED. The fibroblasts from the CED patients show undetectable *Ift144* and the reduction in cilia abundance and length (109).

Currently, two ENU induced mouse mutant models of *Ift144* (Ift144^{twt} and Ift144^{dmhd}) have been generated (160, 161). Mice with the *Twinkle-toes* mutation (Ift144^{twt}), which introduces a leucine-to-proline substitution at amino acid position 750 (L750P, within the first TPR repeat), are partial loss-of-function mutations. Similar to the phenotype of CED patients, Ift144^{twt} embryos die at E11.0 and display polydactyly, small rib cage, and severe craniofacial anomalies. The number of ciliated cells was reduced in Ift144^{twt} mouse limbs and isolated MEFs, while the cilia structure appeared relatively normal. In addition, Ift144^{twt} cells and tissues have enhanced ligand-independent Hh signaling, but reduced response to Hh ligands.

A more severe allele of the *Ift144* mutation is known as *diamondhead* (Ift144^{dmhd}), which represents a functional null mutation (161). These mutant embryos displayed different phenotypes when compared to Ift144^{twt} mice. The cilia were shorter and showed highly disrupted axoneme in Ift144^{dmhd} embryos. Unlike Ift144^{twt}, Ift122^{sopb} and Ift139^{alien}, Ift144^{dmhd} had less activity in Shh signaling, but greater numbers of cells with an intermediate level of Shh activity in the caudal neural tube (161). Ift144^{dmhd} showed smaller forelimb paddle, with truncation in the proximal-distal (PD), and to a lesser extent, the anterior-posterior (AP) axes when compared to those Ift144^{twt} mice revealed a dose-dependent effect of Ift144 on limb outgrowth (160).

The cilia in double mutation of Ift144^{twt} and Ift122^{sopb} (Ift144^{twt}Ift122^{sopb}) were shorter and more bulbous cilia than those in either single mutation and were similar to those in Ift144^{dmhd} embryos (161). Also the phenotype of Ift144^{twt}Ift122^{sopb} is close to that in Ift144^{dmhd}, suggesting that both Ift144^{twt}Ift122^{sopb} and Ift144^{dmhd} result in a stronger disruption of the IFT-A complex. Double mutations of Ift144^{twt} and Dync2h1^{mmi} (Ift144^{twt}Dync2h1^{mmi}) partially rescued the axoneme structure and reduced the level of cilia swollen in Dync2h1^{mmi} (161). The authors concluded that Ift144 is also required for normal anterograde trafficking (161). Further studies on the Hh pathway showed that transportation of the Shh pathway proteins Gli2, SUFU, and Kif7 were normal in Ift144^{twt}, Ift144^{twt}Ift122^{sopb} and Ift144^{dmhd}. But the membrane proteins Arl13b, adenylyl cyclase III (ACIII), and Smo failed to localize to primary cilia in the more complete Ift-A mutation (Ift144^{twt}Ift122^{sopb} and Ift144^{dmhd}). Reduced ACIII level in cilia led to the decrease in cAMP and protein kinase A (PKA) activity, which leads to the ligand independent activation

of Shh. This can explain the up-regulated Shh observed in Ift144^{twt}, but loss of Shh activity in Ift144^{dmhd} with the null mutation of Ift144 due to severe disruptions of the cilia structure and membrane protein trafficking (161).

5.2.4. WDR35 (Ift121)—WDR35 (WR repeat domain 35), which is orthologous to Ift121 in mammals, has seven closely spaced WD40 repeats at the N-terminal and a TRP-like motif at the C-terminus (34). WD40 repeats are believed to have the functions of intracellular trafficking, cargo recognition, and binding. Mutation of this structure caused SRP with a ciliogenesis defect (34). Mutations in the C-terminal domains are more likely associated with CED and result in impairment, but not in complete inhibition of retrograde transport (34, 136).

Mill *et al* isolated a WDR35 null mutant mouse line *yeti* (WDR35^{yet}) from a recessive ENU mutagenesis screen that was looking for genetic effects on embryogenesis (34). They found that a single G>A mutation in the splice acceptor site of exon 22 of *WDR35* resulted in nonsense-mediated decay of mutant transcripts and complete loss of function (34). WDR35^{yet} embryos died at E12.5 and exhibited severe defects in cardiovascular, embryo turning, and limb outgrowth and patterning. Additionally, WDR35^{yet} displayed failure of the somite derivatives, including migration and differentiation of putative ribs (34).

WDR35 accumulates in the basal body and along the cilia axoneme. Both WDR35^{yet} MEFs and fibroblasts from SRP patient (WDR35$^{\Delta 5/\Delta 5}$) had cilia loss and less Ift88 accumulation around the basal body area (34). Interestingly, fibroblasts from CED patient (WDR35 mutation) displayed shorter cilia and accumulation of Ift88 and Ift57 in the distal ends of cilia (135). Those data suggest that *WDR35* mutation in SRP may interfere with anterograde transportation or other vesicular trafficking, which leads to the cilia defect, while the *WDR35* mutation in CED only affects retrograde transport and results in a typical Ift-A mutation phenotype like the *Ift122* mutation (34). Mill *et al* also described WDR^{tm2a} mice as an embryonic stem cell derived “targeted trap” null mutation (34). The loss of WDR35 by targeted mutation phenocopies the WDR35^{yet}, but the details have not yet been revealed (34).

5.2.5. Ift43—Ift43 is the smallest member in Ift-A complex and it does not contain any identifiable domains (28). *Ift43* was the third gene identified as mutation in patients of CED with a homozygote N-terminal deletion (135). A recent study suggested that there is the direct interaction between Ift43 and Ift121, and Ift121 is another gene responsible for CED (90). Fibroblasts from an *Ift43* mutant CED patient had shorter cilia and an accumulation of complex B proteins in the distal ends of cilia indicated by Ift88 and Ift57 staining, which is similar to other Ift-A mutation (135). No *Ift143* mutant mouse model has been published yet.

5.2.6. Ift140—The structure of Ift140 is similar to Ift144 (28). Mutation of *Ift140* has been correlated with MSS and JATD (111). Fibroblasts from some MSS patients had fewer ciliated cells and a normal distribution of Ift140, but altered distributions of Ift88 and Ift46 (evenly distributed along the cilium instead of localizing in the base and tip), suggesting a defect in retrograde ciliary transport (111).

Jonassen *et al* generated Ift140$^{flox/flox}$ mice with two Loxp sites flanking exon 7 of *Ift140* (162). Ift140^{null} was generated by crossing these mice with C57Bl/6 Prm-Cre (Cre recombinase expressed in the germline). These mice died at mid-gestation, but the phenotype has not described yet (162). The function of Ift140 in kidney development has been studied by crossing Ift140$^{flox/flox}$ mice with HoxB7-Cre to delete *Ift140* in the collecting ducts. Loss of Ift140 from the collecting ducts disrupted cilia assembly and caused renal cystic disease. Significant increases in tissue fibrosis and the expression of canonical Wnt pathway genes and Hh mediators was also found in highly cystic, but not precystic, kidneys in these mice, suggesting that abnormalities in these different pathways may influence cyst progression (162).

Another Ift140 mouse model was identified from a comprehensive phenotype-driven ENU screen and was named *cauliflower* (*cauli*) (163, 164). *Cauli* mutation is a recessive missense mutation with a T-to-A substitution in exon 19 at position 2564 (leading to an isoleucine to lysine amino acid change at position 855, p.I855K). Ift140^{cauli} embryos died at E13.5 and exhibited exencephaly, anophthalmia, severely disorganized ribs with extensive exostoses, vertebral and palatal defects, agenesis/hypoplasia of the craniofacial skeleton, and polydactyly of the hindlimbs (163, 164). Cilia morphology in Ift140^{cauli} limb buds was severely disrupted with a broader and bulbous appearance. Similar to other Ift-A mutants, ectopic Hh signaling activity has been observed in Ift140^{cauli} embryos. The loss of Ift140 resulted in reduced Gli3 repressor production, and thus led to the polydactylous phenotype and rib exostoses (164). The null mutation of *Ift140* (Ift140$^{-/-}$) was also generated by Miller *et al* by crossing the Ift140$^{flox/flox}$ mice with CMV-Cre mice (Cre recombinase is expressed in all tissues including germ cells) (164). Ift140$^{-/-}$ embryos died at about E11.5 with the identical phenotype to that observed in Ift140^{cauli} (164).

5.3. Mouse models of Ift complex B proteins

Ift complex B contains 14 known proteins named Ift20, Ift22, Ift25, Ift27, Ift46, Ift52, Ift54, Ift57, Ift70, Ift74/Ift72, Ift80, Ift81, Ift88, and Ift172. *In vitro* and *in vivo* studies examining these proteins are described in the following sections (Table 3).

5.3.1. Ift80—Ift80 is a 777-residue protein, which contains seven WD40 domains (165) and is the first Ift protein that was identified with mutation in human diseases -JATD and SRP type III, (130). Knockdown of ift80 in zebrafish resulted in cystic kidneys with down-regulated Ptch1, suggesting reduced Hh activity (165). Rix *et al* generated the mouse model named Ift80$^{gt/gt}$ using gene trap strategy (insert gene-trap cassette pGT0lxr in the intronic region downstream of exon 9 in Ift80) (70). The homozygotes Ift80$^{gt/gt}$ are hypomorphs with the low level of wild-type transcript production, but most died perinatally. Two percent of homozygotes survived to postnatal stages and had severe growth retardation with short long bones, a narrow rib cage and polydactyly. MEFs from Ift80$^{gt/gt}$ E14.5 embryos had normal cilia but reduced Hh activity in response to smoothened agonist purmorphamine. These data suggested that a low level of Ift80 expression is enough for ciliogenesis, but not sufficient for Hh signaling transduction (70).

The results from our laboratory showed that Ift80 was highly expressed in mouse long bone and skull, as well as during osteoblast and chondrocyte differentiation (166, 167). We used RNA interference (RNAi) to silence *Ift80* in the murine mesenchymal progenitor cell line C3H10T1/2 and bone marrow derived stromal cells (BMSCs) and found that loss of Ift80 led to shorten or loss of cilia and significantly blocked osteogenesis. Gli2 expression was significantly decreased in Ift80-silenced cells, suggesting the impaired Hh pathway activity (167). Silence of Ift80 in BMSCs also impaired the chondrogenic differentiation by down-regulating Hh signaling, whereas up-regulating Wnt signaling (166). Those data suggested the important role of Ift80 in skeletal development. Currently, we have generated $Ift80^{flox/flox}$ conditional knockout mouse alleles, and are identifying the role and mechanism of Ift80 in different bone cells by using specific bone cell Cre transgenic lines to delete Ift80 in various bone cells.

5.3.2. Ift88—Ift88 (Tg737 or Polaris), a TPR-containing protein, was first identified in ARPKD (168). The $Ift88^{Tg737Rpw}$ (also known as ORPK, FVB/N strain) mouse model was generated 20 years ago as a model for human recessive polycystic kidney disease (168). $Ift88^{Tg737Rpw}$ has a transgene insertion-induced hypomorphic allele of Ift88 (continued expression of alternatively spliced transcripts and presence of low levels Ift88), which allows homozygous mutant mice to survive into young adulthood. $Ift88^{Tg737Rpw}$ mice have scruffy fur, severe growth retardation, cystic renal phenotype, and preaxial polydactyly in all limbs (168, 169). $Ift88^{Tg737Rpw}$ mice also have defects in skeletal patterning and growth with craniofacial abnormalities, cleft palate, unfused tibia and fibula (170). The cilia are not completely abolished in $Ift88^{Tg737Rpw}$ but are stunted and malformed (169). Fibroblasts isolated from $Ift88^{Tg737Rpw}$ mice do not respond to platelet-derived growth factor A (PDGF-A) and fail to conduct chemotaxis toward PDGF-A (169). The growth plates of $Ift88^{Tg737Rpw}$ mice are significantly smaller in length and width, suggesting the role of Ift88/cilia in chondrocyte differentiation and hypertrophy (171). Chondrocytes from $Ift88^{Tg737Rpw}$ mice have a defect in the compression-induced Ca^{2+} signaling but not ATP release, suggesting that cilia are involved in ATP reception instead of initiation of mechanotransduction (172).

To further study the function of Ift88, Murcia *et al* (91) generated a null allele ($Tg737^{\Delta 2-3\beta Gal}$ or $Ift88^{tm1Rpw}$, FVB/N strain) by homologous recombination in ESCs. The initial coding exons (exon 2 and part of exon 3) were replaced with the β-galactosidase (β-Gal) reporter gene. $Tg737^{\Delta 2-3\beta Gal}$ embryos that are arrested in development at mid-gestation exhibit neural tube defects, enlargement of the pericardial sac, and significant left-right asymmetry defects. Cilia were absent in $Tg737^{\Delta 2-3\beta Gal}$ ventral node cells. Expression of both *Shh* and *Hnf3β* is reduced in the midline in E8.0 $Ift88^{\Delta 2-3\beta Gal}$ embryos, contributing to the alterations in midline development (91). However, Zhang *et al* found that no changes in Shh or its downstream genes occurred in the limb buds of $Tg737^{\Delta 2-3\beta Gal}$ embryos (170).

Huangfu *et al* identified $Ift88^{fxo}$ (*Flexo*, also called $Ift88^{hypo}$) from the screen of ENU-induced embryonic abnormalities (56). $Ift88^{fxo}$ is a null allele of *Ift88* with deletion of exon 16 (including part of one of the ten predicted TRP motif). $Ift88^{fxo}$ embryos lack nodal cilia and display an unusually sharp angle of the mesencephalic flexure at E9.5.–10.5. Those embryos are arrested at E12.5–13.5 with abnormal brain morphology and preaxial

polydactyly (56, 173). Liu *et al* studied the Hh signaling in the limbs of Ift88^{fxo} embryos and proposed that both Gli activator function (down-regulation of *Ptch1* and *Gli1* expression) and Gli repressor function (*Hand2* misexpression and polydactyly) are compromised in the limbs of Ift88^{fxo} (173).

Haycraft *et al* generated Ift88$^{flox/flox}$ conditional allele with LoxP sites flanking exons 4–6 (174). The deletion of these exons with Cre-line is predicted to result in a translational frame shift and loss of all Ift88 function (a null mutation). Prx1-Cre (Ift88$^{flox/flox}$; Prx1-Cre, limb mesenchyme with both chondrocytes and perichondrium) and Msx2-Cre (Ift88$^{flox/flox}$; Msx2-Cre, limb ectoderm) were used to delete *Ift88* on different cell populations within the developing limb (174). Disrupted Ift88 using both Cre lines caused cilia loss (93, 174). Ift88$^{flox/flox}$; Msx2-Cre mice did not exhibit an overt effect on limb patterning. However, Ift88$^{flox/flox}$; Prx1-Cre displayed severe polydactyly and defects in endochondral bone formation with aberrant Shh and Ihh signaling (174). Song *et al* crossed Ift88$^{flox/flox}$ mice with Col2α1-Cre to delete *Ift88* in committed chondrocyte lineage (Ift88$^{flox/flox}$; Col2α1-Cre) (93). The phenotype of Ift88$^{flox/flox}$; Col2α1-Cre is similar to Kif3a$^{flox/flox}$; Col2α-Cre with postnatal dwarfism and complete loss of the growth plate, resulting from down-regulated the proliferation and up-regulated hypertrophic differentiation of the chondrocytes. They further demonstrated that Ift88 regulated chondrocyte rotation to maintain the columnar organization of the growth plate (93). Chang *et al* studied the signaling pathways involved in the growth plate abnormality by comparing gene expression profiles in normal and Ift88$^{flox/flox}$; Col2α-Cre growth plates (175). They found that the expression of Hh and secreted frizzled-related sequence protein 5 (Sfrp5) (an extracellular antagonist of Wnt signaling pathways) was significantly lower in Ift88$^{flox/flox}$; Col2α-Cre. These data support the increase of Wnt/β-catenin signaling in flat columnar cells of the growth plate in Ift88$^{flox/flox}$; Col2α-Cre as measured by expression of *Axin2* and *Lef1*, as well as nuclear localization of β-catenin (175). In addition, Ift88$^{flox/flox}$; Col2α-Cre mice showed thicker articular cartilage with increased cell density, which probably results from the reduced apoptosis rate in cartilage remodeling (176). The mechanical properties of cartilage from Ift88$^{flox/flox}$; Col2α-Cre mice significantly decreased, particularly in the deeper zones (172). Up-regulation of Hh signaling as measured by expression of *Ptch1* and *Gli1* was observed in Ift88$^{flox/flox}$; Col2α-Cre articular cartilage, which contributes to the osteoarthritis (OA) symptoms. A reduction in the Gli3 repressor to activator ratio also occurred, which is an explanation for the elevated Hh signaling (176).

5.3.3. Ift172—Ift172 is the largest Ift protein. It is predicted to have N-terminal WD-40 repeats and C-terminal α-helical TPRs (28).

Huangfu *et al* identified a *wimple* (*wim*) mutation of Ift172, a null mutation, in a screen for recessive ENU-induced mutations (56). The T to C mutation in the *wim* allele causes a leucine to proline substitution (Leu1564Pro) near the C-terminus. Ift172^{wim} embryos have morphological abnormalities at E9.5 and arrest at E10.5–11.5 due to strong defect in Shh signaling. Ift172^{wim} mice lack nodal cilia and have an open neural tube in the head, which does not have the normal groove on the ventral midline (56). Ptch1 mutant mice (177) (partial exon 1, and exon 2 of ptch1 were replaced with lacZ and a neomycin (neo) resistance gene through homologous recombination in ESCs) were crossed with Ift172^{wim} to

generate double mutants, which showed the similar phenotype as Ift172^{wim}. Loss of Ptch1 caused the activation of Hh pathway, but Ift172 mutation blocked this activation, suggesting Ift172 acts downstream of Ptch1 in Shh signaling pathway (56). The loss of cilia did not affect the response of the Ift172^{wim} mid-gestation embryos or MEFs to Wnt ligands (178).

Friedland-Little *et al* identified Ift172^{avc1} from a screen of ENU-induced mutations (92). This mutation is an A-to-G transition in the splice donor site downstream of exon 24 of Ift172 to alter Ift172 splicing. Ift172^{avc1} allele maintains some wild-type transcript, which is a partial loss of function mutation and dies at birth. Ift172^{avc1} mice show anomalies in vertebral, trancheoesophageal and limb, and defects in cardiac, anal atresia, renal dysplasia and hydrocephalous. But left-right axis formation is normal in Ift172^{avc1} (92). Ift172^{avc1} cells have truncated cilia (including disrupted IFT88 localization) both *in vivo* and *in vitro*. Ift172^{avc1} embryos display a global reduction in the expression of *Ptch1* and *Gli1*. A 70.7% reduction of Gli3 processing (from full-length to transcriptional repressor) in Ift172^{avc1} embryos and disrupted Hh-dependent Gli2 localization in Ift172^{avc1} MEFs has been observed, which contributes to the Hh signaling defect in Ift172^{avc1}. Quantitative analysis wild-type, Ift172$^{avc1/avc1}$ and Ift172$^{wim/avc1}$ revealed the dose-dependent requirement for Ift172 in ciliogenesis and Hh signaling (92).

Another mouse model named *Slb* mutant (Ift172^{Slb}) was generated by Gorivodsky *et al* (179). A *neo* cassette was inserted to replace the first three exons of *Ift172* and cause the loss of function mutation. Ift172^{Slb} mice die between E12.5 and E13.0 with severe craniofacial malformations, defects in brain patterning, failure to close neural tube and exencephaly. Cilia are initiated but shorter and without visible microtubules. Expression of *Shh* and *Gli1* is lower in the developing forebrain and midbrain of Ift172^{Slb}. In addition, Ift172 is required for early regulation of *Fgf8* at the midbrain-hindbrain boundary (179).

To further study the role of Ift172 in the later stage of development, Howard *et al* generated mice with a conditional knockout of Ift172 (Ift172$^{f/f}$) using LoxP sites flanking exons 2–3 (180). Deletion with the Cre line can remove about a third of a WD40 repeat domain and cause a frame shift, resulting in a stop codon. Similar to Ift172^{wim} and 172^{Slb}, germline deletion with CMV-Cre (Ift172$^{\Delta/\Delta}$) leads to embryonic lethality due to neural tube defects. To examine tissue-specific function of Ift172, Prx1-Cre was used to delete Ift172 in the developing limb. Ift172$^{f/t}$; Prx1-Cre mice (one allele is a germ line deletion and another is only deleted in the developing limb bud mesenchyme) have eight digits on each forelimb and a single extra digit on each hind limb (180).

5.3.4. Ift20—Ift20 is the smallest Ift protein in the Ift family and has several unique features. It is the only Ift protein that localizes to the Golgi complex in mammalian cells, suggesting its role in the ciliary protein sorting (165, 166). Ift20 is anchored to the Golgi complex by the Golgi protein-Golgi Microtubule Associated Protein 210 (GMAP210)/ thyroid hormone receptor interacting protein 11 (TRIP11) (166). Without GMAP210, Ift20 is no longer localized to the Golgi structure and cilia are shorter with reduced ciliary localization of membrane protein polycystin-2. GMAP210 mutant mice die at birth and display growth restriction, ventricular septal defects of the heart, omphalocele, and lung hypoplasia (166). Strong knockdown of Ift20 in mammalian cells blocks cilia formation

while moderate knockdown does not block cilia assembly, but reduces the amount of polycystin-2 to localize to the cilia (165). Those data demonstrated GMAP210 and Ift20 work together at Golgi in sorting or transporting proteins like polycystin-2. Besides GMAP210/ TRIP11, Ift20 also exhibits a strong interaction with Ift57/Hippi and kinesin II subunit, Kif3b (181). Ift20 is tethered by Ift57 to the Ift particle, physically interacts with Kif3b and mediates the ATP-dependent dissociation of kinesin. Loss of Ift57 leads to the disassociation of Ift20 from Ift particles but does not affect the association of kinesin to the Ift particle (182).

In addition, Ift20 is expressed in lymphoid and myeloid cells, which do not have primary cilia. Ift20 takes part in the polarized recycling of the TCR/CD3 complex, which is the first connection of Ift proteins and membrane trafficking in cells without cilia (167). But whether Ift20 functions in membrane trafficking in the ciliated cells remains unknown.

The mouse floxed allele of Ift20 ($Ift20^{Flox}$), which has LoxP sites flanking exons 2 and 3 of *Ift20*, has been established by Jonassen *et al* (183). Germline deletion of *Ift20* using Prm-Cre led to embryonic lethality (183). So far, HoxB7-Cre and human red/green pigment gene promoter (HRGP)-Cre have been used to study the function of Ift20 in kidney and photoreceptor cells (183, 184). But the function of Ift20 has yet to be reported in bone, and our lab is currently trying to understand the function and mechanism of Ift20 in bone development and remodeling.

5.3.5. Ift25—Ift25 is one of the two Ift proteins (Ift25 and Ift27) that are absent from *C. elegans* and *Drosophila*, suggesting a role of Ift25 beyond ciliogenesis (185). Keady *et al* generated the $Ift25^{neo}$ mice by using homologous recombination to modify ESCs containing a splice acceptor, a promoterless β-galactosidase-neo resistance gene fusion and LoxP sites flanked exon 3 (185). By crossing these mice with the germ line Cre Prm-Cre mice, they generated $Ift25^{null1}$, which lacks exon 3 of Ift25. Both $Ift25^{neo}$ and $Ift25^{null1}$ are null mutations without Ift25 expression. These mice die at birth with severe heart defects but have normal cilia. These are different from other Ift-B null mutants that usually fail to form cilia and die around mid-gestation. In addition, mutation of Ift25 leads to omphaloceles, polydactyly with a preaxial digit duplication, micrognathia, cleft palate, and malalignment of the sternal vertebrae. Ift25 is needed for the exit of Smo and Ptch1 from cilia (not import) and Gli2 accumulation at the ciliary tip in response to activation of the Shh pathway. Loss of Ift25 leads to a failure to activate the Hh pathway upon stimulation (185).

5.3.6. Ift27—Ift27 belongs to the small G protein family (close to Rab subfamily) with Rab-like small GTPase activity (186, 187). It binds weakly with GDP and GTP, and displays very low, but significant intrinsic GTPase activity (186). In addition, it forms a sub-complex with Ift25 in green algae, *Chlamydomonas reinhardtii*, mice and humans (186, 188). Ift25 and Ift27 seem to be preassembled before entering the cilia and associating with other Ift-B members, suggesting the role of Ift25/27 in Ift initiation (186, 188). However, the roles of the Ift27 in cilia formation and bone development are not yet known and no Ift27 mutant mouse model has been published yet.

5.3.7. RabL5 (Ift22)—Ift22, another Ift protein with significant sequence similarity to Rab-like GTPases, is known as Rab-like 5 (RabL5) in mammals (28). Mutation of the *Ift22* ortholog in *C.elegans* (Rab-like 5) did not alter the cilia (189). But knock-down of Ift22 by RNAi in the trypanosome flagellum surprisingly resulted in short flagella filled with a high amount of IFT proteins, which is a typical retrograde Ift defect phenotype (190). No mouse model or related human diseases have been reported yet.

5.3.8. Ift46—Even though Ift46 does not contain any recognizable domains or motifs, it directly interacts with Ift52, Ift70 and Ift88 in the core of Ift-B (28). Study showed that Ift46 is necessary for Ift-B stability (191). Recently, Ift46 has been identified as a BMP-2 sensitive protein in mouse chondrocytes (192). Ift46 is located in the mouse primary cilium of chondrocytes and is preferentially expressed in early hypertrophic chondrocytes in the growth plate. Knockdown of Ift46 in cultured chondrocytes by small interfering RNA (siRNA) oligonucleotides does not affect the expression of the *Col2α1, Col10α1,* BMP receptors, and Smads. Instead, it up-regulates *Msx1, fibroblast growth factor receptor-1* (*Fgfr1*), *type XII collagen* (*Col12α1*), *biglycan* (*Bgn*), *matrix metalloproteinase-10* (*Mmp10*), and *heat shock protein 47* (*Hsp47*) expression (192). Antisense morpholino oligonucleotides were injected into *Danio rerio* embryos to deplete zebrafish Ift46, which led to severe defects in embryonic development. These data highlight the role of Ift46 in chondrocyte function and vertebrates development (192). However, whether Ift46 is involved in cilia formation in chondrocytes and how it affects bone development and remodeling have not been evaluated yet.

5.3.9. Ngd5 (Ift52)—Ift52 is predicted to have an N-terminal ‘GIft’-domain (GldG/Ift) and proline-rich stretch (28). Ift52 can bind Ift70 and Ift88 directly through the proline-rich stretch (28). Mouse *Ngd5* is the mammalian ortholog of *Ift52* (181). Liu *et al* generated $Ift52^{hypo}$ from two mutant ESC lines in which the *Ngd5* gene was disrupted by replacing it with the lacZ gene (173). The C-terminal 99 amino acids of the Ngd5 protein were replaced with lacZ in the first line (XL826). In the second allele (RRJ295), the last 47 amino acids of the Ngd5 protein were replaced with lacZ. Mice derived from both lines are termed as $Ift52^{hypo}$. They are partial loss-of-function mutations and have similar phenotypes, including tight mesencephalic flexure, left-right and ventral midline defects, polydactyly and craniofacial defects at embryonic stage (173). In addition, *ptch1* is not detected in the limb buds of $Ift52^{hypo}$, suggesting the disruption of Hh signaling (173).

5.3.10. Traf3ip1 (Ift54)—The homology of Ift54 in mammalian systems is tumor necrosis factor alpha receptor 3 interacting protein 1 (Traf3ip1)/microtubule interacting protein that associates with Traf3 (MIP-T3, hereafter called Traf3ip1), which was initially characterized through its interactions with tubulin, actin, TNFR-associated factor-3 (Traf3), interleukin-13 receptor α1 (IL-13R1), and Disrupted-In-Schizophrenia 1 (DISC1). Traf3ip1 inhibits IL-13–mediated phosphorylation of signal transducer and activator of transcription-6 (STAT6). Traf3ip1 also regulates Traf3 and DISC1 by sequestration of these factors to the cytoskeleton in mammals (193, 194).

Berbari *et al* generated the $Traf3ip1^{GT}$ mouse model with embryonic stem cell line harboring a gene trap insertion in intron 11 of Traf3ip1 (193). MEFs from $Traf3ip1^{GT}$ had

nearly 90% less transcript levels than the level in wild-type MEFs. Traf3ip1^{GT} mouse is lethal at the embryonic stage before E13.5, having neural developmental defects, cardiac edema, and polydactyly. Hh signaling was dramatically reduced in both the neural and endoderm tubes in E10.5 Traf3ip1^{GT} embryos as determined by crossing with Ptch1-lacZ Hh reporter mice. By crossing those mice with BAT-Gal Wnt reporter mouse line, the author found that there is no overt alternation in canonical Wnt signaling in the Traf3ip1^{GT} mutant embryos. MEFs from Traf3ip1^{GT} embryos have defective cilia formation, up-regulated acetylated microtubules, and increased cell size. Interestingly, deletion of Traf3ip 1 increases the activity of the mammalian target of rapamycin (mTor) pathway, which likely causes the change of cell size in Traf3ip1 mutant cells (193).

5.3.11. Hippi (Ift57)—Ift57 has a coiled-coil domain at the C-terminus and interacts with Ift20 in a yeast two-hybrid assay (181). The ortholog of *Ift57* in mouse is *Hippi* (*huntingtin interacting protein-1 protein interactor*), which is involved in neuronal apoptotic cell death in Huntington disease (195). Houde *et al* generated Hippi-null mice (Hippi$^{-/-}$, C57BL/6J-129S1/SvImJ genetic background) by replacing the first 95 codons of the *Hippi* open reading frame with the neo gene or neo plus β-Gal (196). Hippi$^{-/-}$ embryos predominantly die prior to E10.5 and have defects in nodal cilia, left–right patterning, and nervous system development. In addition, the expression levels of *Shh* and *ptch1* in the neural tube are down-regulated, suggesting that deletion of Hippi likely disrupts Hh signaling pathway (196).

5.3.12. Ift70—Ift70 is predicted to contain a number of TPRs (28). Mutations of the Ift70 orthologs *dyf-1* in *C. elegans* or *fleer* in zebrafish led to defective cilia formation (197–199). The roles of Ift70 in mouse and human disease have not been reported yet.

5.3.13. Ift74/72 and Ift81—Ift74 and Ift72 are derived from the same gene and often named as Ift74/72 (88). Both Ift74/72 and Ift81 are core proteins in complex B. Ift74/Ift72 interact with the Ift81. They all have coiled-coil regions in their structure (28). Very recently, Bhogaraju *et al* demonstrated that Ift74 and Ift81 form a tubulin-binding module, which is required for ciliogenesis in human RPE-1 cells (retinal pigment epithelium cells), suggesting Ift74/Ift81 play a role in the tubulin transportation within cilia (200). Further studies are needed to determine whether these Ift proteins are involved in bone development.

5.4. Mouse models of Ift motors

Anterograde and retrograde Ift are operated by two types of MT-based motors, kinesin-2 (plus end-directed MT motor) and dynein-2 (minus end-directed MT motor). Although significant efforts have been contributed to elucidate the function of Ift motors (See review (201)), their roles in ciliogenesis and signaling transduction are still poorly characterized (Tables 4=5).

5.4.1. Dynein-2—The dynein motor protein family contains axonemal dynein, cytoplasmic dynein-1, and cytoplasmic dynein-2, which are involved in a wide range of functions in eukaryotic cells (See review (202)). Dynein-2 only exists in the organisms that have cilia or eukaryotic flagella and is believed to function primarily as the retrograde motor for Ift (202).

Dynein-2 contains a heavy chain (DYNC2H1), an intermediated chain (D2IC), a light intermediate chain (D2LIC, or LIC3), and a light chain (LC) (201, 203). The mouse homology of LC and D2IC has not been reported, and how the Dynein-2 motor interacts with Ift protein complexes is largely unknown.

5.4.1.1. DYNC2H1: Dync2h1 encodes the heavy chain of the cytoplasmic dynein-2 motor (DYNC2H1, or DHC1b and DHC2) (35). The Dync2h1 mutation has been linked to the JATD and SRP (33, 35, 131). Chondrocytes from patients with Dync2h1 mutation had short cilia with bulbous distal ends (33).

Huangfu *et al* generated two mouse lines with Dync2h1 mutation named Dnchc2^{lln} and Dnchc2^{GT} (48). Dnchc2^{lln} is ENU induced mutation with a phenylalanine-to-serine (F3890S) mutation in a conserved residue of the Dnchc2 motor domain. Dnchc2^{GT} is generated by using the ESC gene trap insertion approach, which produces a truncated Dync2h1 (lacking the entire dynein motor domain) fused to β-geo (48). Homozygous Dnchc2^{lln}, Dnchc2^{GT}, and transheterozygous Dnchc2^{lln}/Dnchc2^{GT} mice all die at approximately E12.5 and have similar phenotypes, including abnormal brain morphology, randomization of heart-looping polarity and polydactylous. Cilia were present on the Dnchc2^{lln} embryos with altered morphology. These cilia are similar to those seen in the Ift-A defect embryos, with reduced length and a bulge along their length (48, 204). Among Dync2h1^{lln}, Dync2h1^{ttn} and Dync2h1^{Gt}, cilia in Dync2h1^{lln} are less affected (204). Hh signaling is disrupted, and the *Ptch1* expression is reduced in Dnchc2^{lln} neural tube. Besides, Hh pathway is fully activated in Ptch1 mutants. Dnchc2^{lln} Ptch1 double mutant mice has the similar phenotypes as Dnchc2^{lln} (48). Smo, Gli2, and Ptch1 accumulate along the Dnchc2^{lln} cilia with or without Shh stimulation (204). These results suggest that Dync2h1 acts downstream of Ptch1.

Dync2h1^{ttn} was generated by Ocbina *et al* also using ENU mutation method (205). Dync2h1^{ttn} carries an A-to-C substitution in the splice donor site upstream of exon 51, which deletes 38 amino acids from the ATPase-activator (AAA) domain 4 (205). Cilia morphology is altered on the Dync2h1^{ttn} MEFs with reduced length and bulges along the axoneme (67). Smo accumulates in the primary cilia of Dync2h1^{ttn} MEFs even in the absence of Shh. But the presence of Smo in cilia is not sufficient to activate the Gli-luciferase reporter, suggesting that retrograde Ift blocks activated Gli2 to move out of the cilia (205). Wnt signaling is normal in mid-gestation Dync2h1^{ttn} embryo or embryo-derived fibroblasts (67).

Besides the above mentioned models, Liem *et al* generated another ENU-induced Dync2h1 mutation mouse line Dync2h1^{mmi} (206). Dync2h1^{mmi} has a missense mutation (I1789N) in the motor domain. Dync2h1^{mmi} has defects in neural tube and motor neurons similar to other Dync2h1 mutants (206). Transmission electron microscopy (TEM) analysis revealed that cilia in Dync2h1^{mmi} are swollen and filled with electron-dense particles (161). Axonemal microtubules in Dync2h1^{mmi} cilia are defective having a reduced number of cilia and singlets instead of doublets (161).

May *et al* identified two independent ENU-induced null mutations, Dnchc2^{Q397Stop} and Dnchc2^{W2502R} (207). Dnchc2^{Q397Stop} carries an early nonsense mutation at amino acid position 397 (an early stop codon). Dnchc2^{W2502R} carries a missense mutation in a conserved AAA domain (position 2502) that is predicted to be required for motor activity. Both Dnchc2^{Q397Stop} and Dnchc2^{W2502R} show similar developmental defects with severe defects in dorsoventral patterning of the forebrain and patterning of the spinal cord (207). Most of the mutant embryos die at E12.0 or earlier with pericardial edema and heart failure. Cilia in mutant embryos are shorter but wider than the normal cilia. Both Gli activator (*Gli1* expression) and Gli repressor activity (*Hoxd13* and *gremlin* expression) are significantly lower. In addition, mutant embryos have a disruption of the Gli3 proteolytic processing and Smo localized to the cilia (207).

Ocbina *et al* studied the relationships between Dync2h1 and other genes required for ciliary trafficking. To investigate the relationship between anterograde ciliary trafficking and Dync2h1, they generated double mutant allele of *Ift172*, an Ift-B gene and *Dync2h1*. The phenotype of Dync2h1^{lln}Ift172^{wim} double mutant is similar to that of Ift172^{wim} (a null mutation allele), showing an absent of cilia and defects in all ventral neural cell types (204). Double mutation of *Dync2h1* and *Ift172* using Ift172^{avc1}, a partial loss-of-function allele of *Ift172*, can partially rescue the Dync2h1^{lln} phenotype. Interestingly, a more dramatic rescue in Shh signaling and cilia morphology is found in the Dync2h1^{lln}Ift172$^{avc1/+}$ double mutants. Dync2h1^{lln}Ift172$^{avc1/+}$ embryos survive to at least E16.5 without having polydactyly. Thus, these results suggest that a modest reduction of Ift-B expression and anterograde trafficking can rescue ciliogenesis and Shh signaling transduction in the absence of Dync2h1 (204). To further elucidate the relationship between retrograde motors and Ift-A proteins, Ift122 from Ift-A was used to generate Ift122 and Dync2h1 double mutant mice. Interestingly, mutants that are homozygous for both Dync2h1^{lln} and Ift122^{sopb}, resemble the Ift122^{sopb} phenotype with similar cilia morphology and ectopic activity of the Shh pathway in the neural tube (204). Ift88 is enriched at the cilia, and Gli2 is limited to the tips of cilia in Ift122^{sopb}Dync2h1^{lln}. However, Smo is only in cilia with Shh stimulation in Ift122^{sopb}Dync2h1^{lln}. Deletion of Ift122 relieves the accumulation of proteins within the cilia caused by loss of Dync2h1, suggesting Ift122 or Ift-A complex plays a role in anterograde as well as retrograde trafficking (204). Ift122^{sopb} leads to the lack of Dync2h1 along the cilia, which may explain why the phenotypes in Ift122^{sopb}Dync2h1^{lln} double mutants are similar to that in the Ift122^{sopb} single mutants. Dync2h1^{lln}Ift122$^{sopb/+}$, which has lowered expression of Ift122, can partially rescue the phenotype of Dync2h1^{lln}, including the cilia morphology, ventral neural development and Shh-dependent protein trafficking in cilia (204), indicating that normal Shh-dependent protein trafficking in cilia can take place in the absence of Dync2h1 if the Ift122 level is reduced.

5.4.1.2. mD2LIC: Mouse dynein-2 light intermediate chain (mD2LIC) was recently discovered. Both reciprocal immunoprecipitations and sedimentation assays showed that mD2LIC interacts specifically with DYNC2H1, suggesting mD2LIC is also involved in retrograde transport (208, 209).

Rana *et al* generated a null *mD2LIC* mutant mice (mD2LIC$^{-/-}$) by disrupting both the transcriptional and translational start sites in *mD2LIC* (210). mD2LIC$^{-/-}$ mice die before

E11.5 with defects in notochord and floorplate formation, a reduction in definitive endoderm and loss of cilia in the node of mD2LIC$^{-/-}$ embryos. mD2LIC$^{-/-}$ embryos displayed reduction in Hh signaling activity, which is similar to the phenotype observed in Smo$^{-/-}$ and Shh$^{-/-}$Ihh$^{-/-}$ double mutants.

5.4.2. Kinesin-2—Kinesins are ATP-dependent microtubule-based molecular motors that carry cargo along microtubules in an anterograde direction (211, 212). There are more than 40 members in the kinesin superfamily that can be divided into 14 distinct families (kinesin-1 to -14) (213). Accumulating evidence shows heterotrimeric kinesin-2 motor is the "core" of IFT motor while other proteins including kinesin-2, -3 and -4 function as "accessory" motors for the transport of specific cargo dependent on cell types (211). In vertebrates, two distinct heterotrimeric kinesin-2 complexes, named kinesin-2 family protein A (Kif3a)/Kif3b/ kinesin-associated protein (KAP3) and Kif3A/Kif3C/ KAP3, which may play different roles in the ciliogenesis and function. In addition, heterotrimeric kinesin-2 and homodimeric Kif17 in the Kinesin-2 family also transport exogenously expressed cyclic nucleotide-gated channels into the cilium (214). Kif7 in the kinesin-4 family is localized to cilia base and the tip in mouse embryos and plays important roles in the ciliary trafficking and the response of Hh signaling (206, 215, 216).

5.4.2.1. Kif3a: Marszalek *et al* generated the Kif3a-Null mouse by removing exon 2 in ESCs, which completely disrupted Kift3a protein expression (94). The Kif3a-Null mouse usually dies at E10 with structural abnormalities, defects in left and right asymmetry, and cilia loss in embryonic node, suggesting that a kinesin-based transport is required for cilia formation (94).

Kif3a$^{flox/flox}$ was generated by inserting two LoxP sites, which flanks exon 2 of *Kif3a* in the intronic DNA sequences (94, 217). By crossing these mice with Wnt1-Cre (Kif3a$^{flox/flox}$; Wnt1-Cre or Kif3a CKO), *Kif3a* is inactive in neural crest lineage cells. Kif3a$^{flox/flox}$; Wnt1-Cre mice die shortly after birth due to respiratory failure and display severe craniofacial defects, including clefting of the secondary palate and widened frontonasal prominence (218, 219). Kolpakova-Hart *et al* reported the Kif3a$^{flox/flox}$; Wnt1-Cre mice have the similar phenotype as Smo$^{flox/flox}$; Wnt1-Cre mice (Shh signaling is disrupted in neural crest cells due to deletion of Smo). In addition, Gli1 is not detectable in the mesenchymal cells. Those data demonstrate that Hh signaling is impaired in Kif3a-deficient neural crest–derived mesenchyme (218). In contrast, Brugmann *et al* found that Kif3a-deficient neural crest–derived facial mesenchyme lacks cilia and has enhanced Hh signaling, including enhanced *Gli1, Ptch1* and *Shh*, but reduced *Gli3*, which accounts for the excessive proliferation in the facial prominences (219). The opposite Hh signaling response after deletion of Kif3a may result from inconsistent expression of Gli proteins in different tissues.

To study the role of Kif3a in axial and appendicular skeleton development, Dermo1-Cre (mesoderm-specific) was used to inactivate Kif3a in the trunk and limb skeletal progenitor cells (Kif3a$^{flox/flox}$; Dermo1-Cre) (218). Kif3a$^{flox/flox}$; Dermo1-Cre mice die immediately after birth, which likely result from the defects in ribcage. Besides, Kif3a$^{flox/flox}$; Dermo1-Cre mice have a split sternum, polydactyly and defects in knee joints and limbs (218).

Restricted deletion of Kif3a in the lateral plate mesoderm with Prx1-Cre (Kif3a$^{flox/flox}$; Prx1-Cre), which is limb/sternum-specific and does not affect the somitic mesoderm skeletal derivatives, such as ribs and vertebrae, leads to abnormal rib pairing, forelimb polydactyly and profound shortening of limb bones (174, 218). Ihh signaling is inactive (reduced *Gli1* expression and normal *Gli3* expression) in the long bone in Kif3a$^{flox/flox}$; Prx1-Cre, which contributes to defects in chondrocyte differentiation and the loss of the bone collar adjacent to the metaphysis (174, 218).

Specific deletion of Kif3a in cartilage using Col2α1-Cre (Kif3a$^{flox/flox}$; Col2α1-Cre) resulted in abnormal cranial base development and altered synchondrosis growth plate organization and function at the postnatal stage. Kif3a deficient synchondroses display a delay in chondrocyte hypertrophy and enhanced intramembranous ossification. Hh signaling is significantly reduced within mutant growth plates but enhanced and widespread in all of the perichondrial tissues in Kif3a$^{flox/flox}$; Col2α1-Cre mice as detected the expression of Ptch1, Gli1, and syndecan-3 (hedgehog-binding cell-surface component) (220). Song *et al* reported that Kif3a$^{flox/flox}$; Col2α1-Cre mice have postnatal dwarfism. Chondrocytes proliferation is reduced, but the hypertrophic differentiation is up-regulated, which leads to premature loss of the growth plate in Kif3a$^{flox/flox}$; Col2α1-Cre mice (93). Moreover, cilia, chondrocyte rotation, actin cytoskeleton and localization of activated FAK are all disrupted, suggesting that an important role of Kif3a or cilia in maintaining the columnar organization of the growth plate and chondrocyte differentiation. In addition, *Ptch1* expression of the Hh signaling pathway is not changed (93).

To analyze the function of Kif3a in osteoblast formation and function, Qiu *et al* used Oc-Cre (osteocalcin promoter, limited in mature osteoblast) to specifically delete Kif3a in the osteoblast linage (Kif3a$^{flox/flox}$; Oc-Cre). Kif3a$^{flox/flox}$; Oc-Cre mice exhibit osteopenia at six weeks of age, which is partially recovered at 16 weeks. Kif3a deficiency leads to a reduction in the number of cilia and their length. Deletion of Kif3a increases cell proliferation but impairs osteoblastic differentiation. Qiu *et al* also found that deletion of Kif3a impairs intracellular calcium response to fluid flow shear stress and reduces Hh and Wnt responses, which may account for the defect of osteoblast-mediated bone formation in Kif3a$^{flox/flox}$; Oc-Cre mice (221). Temiyasathit *et al* generated another osteoblast linage mutant mouse line (Kif3a$^{flox/flox}$; Kif3a; Colα1(I)) using the Col1α 2.3-Cre (2.3kb fragment of the α1(I)-collagen promoter, deletion in osteoblast progenitor cells) mice (222). Kif3a; Colα1(I)-Cre mice have no obvious skeletal defects. However, Kif3a; Colα1(I)-Cre mice exhibited reduced bone formation in response to mechanical ulnar loading, which linked the Kif3a/cilia to mechanosensor function in the bone (222).

Kinumatsu *et al* studied the role of Kif3a/cilia in temporoman-dibular joint (TMJ) development (223). Three-month-old Kif3a; Col2α1-cre mice had narrow and flat condyles with an irregular bony surface that was often fused with the articular disc. Alteration of Ihh signaling topography was associated with ectopic bone formation in condyles, implicating Kif3a/cilia are required for the coordination of Hh in chondrogenic condylar growth (223).

5.4.2.2. Kif3b: Kif3b is the other motor subunit in kinesin-2. A recent study suggested the Kif3b serves as a link between polycystin-2 (PC2, encoded by *PKD2*) and fibrocystin/

polyductin (FPC, encoded by *PKHD1*, which is responsible for ARPKD), and mediates the regulation of PC2 channel function by FPC (224).

Nonaka *et al* generated the Kif3b-Null mutant mouse model by replacing most of the first exon (encoding the entire kinesin motor domain) with neo cassette (225). Kif3b-Null embryos die at mid-gestation and exhibit randomized left–right asymmetry, growth retardation, pericardial sac ballooning, and neural tube disorganization. Cilia is completely absent in the nodes of Kif3b-Null embryos.

5.4.2.3. Kif7: Kif7 is the mammalian homologue of *Drosophila* Costal2 (Cos2), which plays a central role in the Hh pathway in *Drosophila* (216, 226). Kif7 belongs to the kinesin-4 family and has an N-terminal motor domain (227). Knockdown of Kif7 in zebrafish resulted in ectopic Hh signaling, suggesting that Kif7 also acts in Hh signal in vertebrates (228).

Cheung *et al* generated the conditional allele of *Kif7* by flanking exons 2–4 with LoxP sites ($Kif7^{flox/flox}$) (215). By crossing $Kif7^{flox/flox}$ with NLS-Cre transgenic mice (ubiquitous Cre expression), they created the null mutation of Kif7 ($Kif7^{flox/flox}$; NLS-Cre), and found that $Kif7^{flox/flox}$; NLS-Cre mice die at birth with severe malformations, including exencephaly, polydactyly, and sternal defects, a phenotype similar to the phenotype of Gli3 mutant mice. They further found that Kif7 physically interacts with Gli transcription factors and controls their proteolysis and stability (215). The deletion of Kif7 up-regulates full-length Gli2 while it down-regulates truncated 83-kD repressor Gli3 in total embryo lysates. To fully understand the role of Kif7 in Hh signaling pathway, they further generated double mutants by using *Smo* mutant, *Gli2* mutant, or *Gli3* mutant mice to cross with $Kif7^{flox/flox}$; NLS-Cre, and compared these mutants with each single mutant. Their results suggested that Kif7 plays a critical role in the balance of Gli activators and repressors downstream of Smo (215).

Liem *et al* identified an ENU-induced *matariki* (*maki*) mutation of *Kif7* ($Kif7^{maki}$) (206). $Kif7^{maki}$ is a missense mutation (L130P) in a conserved region of the motor domain of *Kif7*, which led to the loss of Kif7 function. $Kif7^{maki}$ mice die at the end of gestation with abnormal motor neurons, preaxial polydactyly and elevated Shh signaling. The results from *Smo* and *Kif7* double mutation result in Shh-dependent ventral neural cell types at E10.5, suggesting that Kif7 functions downstream of Smo and that loss of Kif7 causes ligand-independent activation of Shh pathway. Loss of Kif7 leads to a reduction in processed Gli3 proteins and in the ratio of processed Gli3/full-length Gli3, confirming the role of Kif7 in Gli3 proteolysis or stability. $Kif7^{maki}$ mice have normal cilia. To study the relationship between Kif7 and cilia, $Ift172^{wim}Kif7^{maki}$ double mutants were generated by Liem *et al* (206). They found that $Ift172^{wim}Kif7^{maki}$ is similar to $Ift172^{wim}$ mutants, suggesting that the activity of Kif7 depends on the presence of cilia. To analyze the role of Kif7 in ciliary trafficking (206), Liem *et al* also generated $Dync2h1^{mmi}Kif7^{maki}$ double mutants and found that $Dync2h1^{mmi}Kif7^{maki}$ phenocopies $Kif7^{maki}$ mutants with greater loss of ventral neural cell types, suggesting that Kif7 functions before retrograde Ift, and that DYNC2H1 has additive and positive roles in Shh signaling (206).

Endoh-Yamagami *et al* generated *Kif7* knockout mice (Kif7-KO) by replacing the initiation codon and following N-terminus motor domain with a neo cassette (216). Kif7-KO embryos

display spinal cord defects, preaxial polydactyly, exencephaly, and microphthalmia, which mimic the phenotypes of Gli3 mutants. The Gli3 repression targets *Gremlin* and *HoxD13* are elevated in Kif7-KO. Meanwhile, *Gli1* and *Ptch1* expression are normal in both Kif7-KO embryos and MEFs. Those data suggest that Kif7 regulates Hh signaling mainly through controlling the formation or function of the Gli3 repressor. Cilia morphology is normal in MEFs from Kif7-KO embryos. Kif7 accumulates at the tip of the cilia in an Hh-dependent manner. Kif7 physically interacts with Gli3 and is required for efficient Gli3 processing to its repressor form, indicating that Kif7 functions principally as a negative regulator of the Hh pathway in mice.

5.4.2.4. Kif17: Kif17 belongs to the kinesin-2 family, and a pair of Kif17 forms a homodimer with their head domain (229). Kif17 has diverse functions in different species and different kind of cells. Dysfunctions of Kif17 are linked to a number of pathologies (See review (229)). Kif17 or its homolog mediates Ift cargos to the ciliary tip, therefore, it plays a role in ciliogenesis and function (229). Recently, a new peptide named TTC308 has been identified in Ift complex B in mouse pituitary cells that interacted with mouse Kif17 in co-immunoprecipitation studies (230). This finding confirmed the possible functional interaction between Kif17 and cargo transport. Whether Kif7 takes part in the ciliogenesis in mice is currently unknown.

Yin *et al* generated Kif7 mutant mice ($Kif17^{-/-}$) by replacing exon 4 of Kif17 with a poly (A)-less PGK-neo cassette (231) resulting in a frame shift, and disruption of Kif17 expression. $Kif17^{-/-}$ mice grow normally without any gross defects. They found that Kif7 is important for maintenance of N-methyl-D-aspartate (NMDA) receptor subunit 2B (NR2B) and NR2A level in hippocampal neurons, which is involved in memory and the learning process. However, whether $Kif17^{-/-}$ mice have the bone related phenotype has not been evaluated yet (231).

6. SUMMARY AND PERSPECTIVES

The development of transgenic and mutagenesis technology provides powerful tools to study the function of cilia, Ift proteins, and motors. Some of the Ift proteins and motors already have the mouse models established. A few of them have more than one model with different degrees of loss of function, allowing the study of dosage dependent effects of these genes. The loss of Ift complex A protein usually leads to the “swollen” cilia, which are filled with complex B proteins, suggesting that the complex B, which is in charge of the anterograde transport, can function without the complex A. Mutations of most Ift complex B proteins lead to cilia disruption due to the totally blocked anterograde transport. This raises the problems to distinguish the function of individual Ift proteins and to identify whether the phenotype results from a deficient Ift protein alone or is secondary to cilia loss. It is also possible that the severe consequence of loss of cilia masks the other function of Ift proteins independent of cilia.

Over the past few years, much attention has been paid to elucidating the gene functions and mimicking the human diseases using mouse models. However, the treatment of Ift- and cilia-related diseases in humans is still at the initial developmental stages. For the patients

with the Ift protein or Ift motor mutation, exogenous introduction of the Ift or Ift-related proteins or gene to treat these diseases are worth trying. However, before doing so, it is necessary to figure out which genes are defective in each individual patient and how these genes interact with other genes in the cells. Currently, several candidate modulators for ciliogenesis and cilium length have been found from one high-throughput functional screening (232). Further studies should elucidate whether these modulators can rescue ciliogenesis and cilia function in Ift proteins/motors defective or mutant cells. Proper dosage and delivery methods could be tested with the described mouse models. We anticipate that those small molecules will provide us novel strategies to treat ciliopathies. More work is needed to achieve the comprehensive understanding of the downstream pathways of cilia. Much attention has been paid to the Hh signaling pathways, but the interactions of Hh signaling and cilia/Ift, and the relationship of cilia/Ift with Wnt, Notch, PDGF and many other pathways are still ambiguous or largely unknown. With better knowledge of these pathways and how they interact with cilia/Ift, proper agonists or antagonists can be selected or developed to regulate the downstream signaling. These mouse models provide the needed tools to test the target candidates for the treatment of the ciliopathies patients.

Acknowledgments

We thank Dr. Kristina Wasson-Blader for editing our manuscript. We apologize to the many researchers whose work could not be cited due to space limitations. Research reported in this publication was supported by the National Institute of Arthritis and Musculoskeletal and Skin Diseases, and National Institute of Dental and Craniofacial Research under Award Numbers AR061052, AR066101 and DE023105 to S.Y. The content is solely the responsibility of the authors and does not necessarily represent the official views of the National Institutes of Health.

Abbreviations

MTs	microtubules
Ift	intraflagellar transport
JATD	Jeune asphyxiating thoracic dystrophy
SRP	short rib polydactyly syndromes
Hh	hedgehog
Ihh	Indian hedgehog
Shh	Sonic hedgehog
Ptch1	Patched 1
Smo	Smoothened
PCP	planar cell polarity
BBS	Bardet–Biedl syndrome
Evc	Ellis-van Creveld syndrome protein homolog
OFD1	oral-facial-digital syndrome 1
MKS	Meckel-Gruber syndrome

JBTS	Joubert syndrome
JSRD	JBTS-related disorder
LCA	Leber congenital amaurosis
PCD	primary ciliary dyskinesia
KS	Kartagener syndrome
NPHP	nephronophthisis
SLS	Senior-Loken syndrome
ADPKD	Autosomal dominant polycystic kidney disease
ARPKD	autosomal recessive polycystic kidney disease
US	Usher syndrome
ALMS	Alström syndrome
MSS	Mainzer-Saldino-Syndrome
ATD	asphyxiating thoracic dystrophy
WAD	Weyers acrofacial dysostosi
NEK1	never-in-mitosis Kinase 1
CED	Cranioectodermal dysplasia
MKS	Meckel syndrome
ENU	N-ethyl-N-nitrosourea
PDGF-A	platelet-derived growth factor A
ESCs	embryonic stem cells
THM1	Tetratricopeptide Repeat Containing Hedgehog Modulator 1
MEFs	mouse embryo fibroblasts
PD	proximal-distal
AP	anterior-posterior
ACIII	adenylyl cyclase III
SUFU	Suppressor of Fused
BMSCs	bone marrow derived stromal cells
Sfrp5	secreted frizzled-related sequence protein 5
OA	osteoarthritis
neo	neomycin
GMAP210	Golgi Microtubule Associated Protein 210
TRIP11	thyroid hormone receptor interacting protein 11

HRGP	human red/green pigment gene promoter
GTPase	guanosine triphosphate hydrolases
Fgfr1	fibroblast growth factor receptor-1
Col12α1	type XII collagen
Bgn	biglycan
Mmp10	matrix metalloproteinase-10
Hsp47	heat shock protein 47 kDa
Traf3	TNFR-associated factor-3
IL-13R1	interleukin-13 receptor α1
DISC1	Disrupted-In-Schizophrenia 1
STAT6	signal transducer and activator of transcription-6
AAA	ATPase-activator
PC2	polycystin-2
TMJ	temporoman-dibular joint
FPC	fibrocystin/polyductin
OSM-3	osmotic avoidance abnormal protein 3
NMDA	N-methyl-D-aspartate
NR2B	NMDA receptor subunit 2B

References

1. Teti A. Bone development: overview of bone cells and signaling. Curr Osteoporos Rep. 2011; 9(4): 264–73. [PubMed: 21948208]
2. Karsenty G, Wagner EF. Reaching a genetic and molecular understanding of skeletal development. Dev Cell. 2002; 2(4):389–406. [PubMed: 11970890]
3. Cooper C, Harvey N, Javaid K, Hanson M, Dennison E. Growth and bone development. Nestle Nutr Workshop Ser Pediatr Program. 2008; 61:53–68.
4. Cancedda R, Descalzi Cancedda F, Castagnola P. Chondrocyte differentiation. Int Rev Cytol. 1995; 159:265–358. [PubMed: 7737795]
5. Colnot C. Cellular and molecular interactions regulating skeletogenesis. J Cell Biochem. 2005; 95(4):688–97. [PubMed: 15880692]
6. van der Eerden BC, Karperien M, Wit JM. Systemic and local regulation of the growth plate. Endocr Rev. 2003; 24(6):782–801. [PubMed: 14671005]
7. Day TF, Yang Y. Wnt and hedgehog signaling pathways in bone development. J Bone Joint Surg Am. 2008; 90(Suppl 1):19–24. [PubMed: 18292352]
8. Zanotti S, Canalis E. Notch regulation of bone development and remodeling and related skeletal disorders. Calcif Tissue Int. 2012; 90(2):69–75. [PubMed: 22002679]
9. Rosen V. BMP2 signaling in bone development and repair. Cytokine Growth Factor Rev. 2009; 20(5–6):475–80. [PubMed: 19892583]
10. Combs CE, Nicholls JJ, Duncan Bassett JH, Williams GR. Thyroid hormones and bone development. Minerva Endocrinol. 2011; 36(1):71–85. [PubMed: 21460788]

11. Smirnov SV, Vasil'eva AB. The role of thyroid hormones in skull bone development in the ribbed newt Pleurodeles waltl (Urodela: Salamandridae). Dokl Biol Sci. 2001; 379:396–8. [PubMed: 12918385]
12. Barlow-Stewart, K. The Australasian genetics resource book : a source of current and accurate information for health professionals, individuals and families, teachers and students. Centre for Genetics Education; 2007.
13. Zelzer E, Olsen BR. The genetic basis for skeletal diseases. Nature. 2003; 423(6937):343–8. [PubMed: 12748653]
14. Makitie O. Molecular defects causing skeletal dysplasias. Endocr Dev. 2011; 21:78–84. [PubMed: 21865756]
15. Badano JL, Mitsuma N, Beales PL, Katsanis N. The ciliopathies: an emerging class of human genetic disorders. Annu Rev Genomics Hum Genet. 2006; 7:125–48. [PubMed: 16722803]
16. Eggenschwiler JT, Anderson KV. Cilia and developmental signaling. Annu Rev Cell Dev Biol. 2007; 23:345–73. [PubMed: 17506691]
17. Michaud EJ, Yoder BK. The primary cilium in cell signaling and cancer. Cancer Res. 2006; 66(13):6463–7. [PubMed: 16818613]
18. Ishikawa H, Marshall WF. Ciliogenesis: building the cell's antenna. Nat Rev Mol Cell Biol. 2011; 12(4):222–34. [PubMed: 21427764]
19. Ruiz-Perez VL, Blair HJ, Rodriguez-Andres ME, Blanco MJ, Wilson A, Liu YN, Miles C, Peters H, Goodship JA. Evc is a positive mediator of Ihh-regulated bone growth that localises at the base of chondrocyte cilia. Development. 2007; 134(16):2903–12. [PubMed: 17660199]
20. Lin F, Hiesberger T, Cordes K, Sinclair AM, Goldstein LS, Somlo S, Igarashi P. Kidney-specific inactivation of the KIF3A subunit of kinesin-II inhibits renal ciliogenesis and produces polycystic kidney disease. Proc Natl Acad Sci U S A. 2003; 100(9):5286–91. [PubMed: 12672950]
21. Haycraft CJ, Zhang Q, Song B, Jackson WS, Detloff PJ, Serra R, Yoder BK. Intraflagellar transport is essential for endochondral bone formation. Development. 2007; 134(2):307–16. [PubMed: 17166921]
22. Koyama E, Young B, Nagayama M, Shibukawa Y, Enomoto-Iwamoto M, Iwamoto M, Maeda Y, Lanske B, Song B, Serra R, Pacifici M. Conditional Kif3a ablation causes abnormal hedgehog signaling topography, growth plate dysfunction, and excessive bone and cartilage formation during mouse skeletogenesis. Development. 2007; 134(11):2159–69. [PubMed: 17507416]
23. Pazour GJ, Rosenbaum JL. Intraflagellar transport and cilia-dependent diseases. Trends Cell Biol. 2002; 12(12):551–5. [PubMed: 12495842]
24. Yoder BK. Role of primary cilia in the pathogenesis of polycystic kidney disease. J Am Soc Nephrol. 2007; 18(5):1381–8. [PubMed: 17429051]
25. Pan J, Wang Q, Snell WJ. Cilium-generated signaling and cilia-related disorders. Lab Invest. 2005; 85(4):452–63. [PubMed: 15723088]
26. KozMINSKI KG, Johnson KA, Forscher P, Rosenbaum JL. A motility in the eukaryotic flagellum unrelated to flagellar beating. Proceedings of the National Academy of Sciences. 1993; 90(12): 5519–5523.
27. Rosenbaum JL, Witman GB. Intraflagellar transport. Nature Reviews Molecular Cell Biology. 2002; 3(11):813–825.
28. Taschner M, Bhogaraju S, Lorentzen E. Architecture and function of IFT complex proteins in ciliogenesis. Differentiation. 2012; 83(2):S12–S22. [PubMed: 22118932]
29. Huber, C.; Cormier-Daire, V. American Journal of Medical Genetics Part C: Seminars in Medical Genetics. Wiley Online Library; 2012. Ciliary disorder of the skeleton.
30. Schwartz RS, Hildebrandt F, Benzing T, Katsanis N. Ciliopathies. New England Journal of Medicine. 2011; 364(16):1533–1543. [PubMed: 21506742]
31. Badano JL, Mitsuma N, Beales PL, Katsanis N. The ciliopathies: an emerging class of human genetic disorders. Annu Rev Genomics Hum Genet. 2006; 7:125–148. [PubMed: 16722803]
32. Baker, K.; Beales, PL. American Journal of Medical Genetics Part C: Seminars in Medical Genetics. Wiley Online Library; 2009. Making sense of cilia in disease: the human ciliopathies.

33. Merrill AE, Merriman B, Farrington-Rock C, Camacho N, Sebald ET, Funari VA, Schibler MJ, Firestein MH, Cohn ZA, Priore MA. Ciliary abnormalities due to defects in the retrograde transport protein DYNC2H1 in short-rib polydactyly syndrome. The American Journal of Human Genetics. 2009; 84(4):542–549.
34. Mill P, Lockhart PJ, Fitzpatrick E, Mountford HS, Hall EA, Reijns MA, Keighren M, Bahlo M, Bromhead CJ, Budd P. Human and Mouse Mutations in *WDR35* Cause Short-Rib Polydactyly Syndromes Due to Abnormal Ciliogenesis. The American Journal of Human Genetics. 2011; 88(4):508–515.
35. Dagoneau N, Goulet M, Geneviève D, Sznajer Y, Martinovic J, Smithson S, Huber C, Baujat G, Flori E, Tecco L. *DYNC2H1* Mutations Cause Asphyxiating Thoracic Dystrophy and Short Rib-Polydactyly Syndrome, Type III. The American Journal of Human Genetics. 2009; 84(5):706–711.
36. Scherft JP, Daems WT. Single cilia in chondrocytes. J Ultrastruct Res. 1967; 19(5):546–55. [PubMed: 6055783]
37. Tummala P, Arnsdorf EJ, Jacobs CR. The role of primary cilia in mesenchymal stem cell differentiation: a pivotal switch in guiding lineage commitment. Cell Mol Bioeng. 2010; 3(3):207–212. [PubMed: 20823950]
38. Malone AM, Anderson CT, Tummala P, Kwon RY, Johnston TR, Stearns T, Jacobs CR. Primary cilia mediate mechanosensing in bone cells by a calcium-independent mechanism. Proc Natl Acad Sci U S A. 2007; 104(33):13325–30. [PubMed: 17673554]
39. Xiao Z, Zhang S, Mahlios J, Zhou G, Magenheimer BS, Guo D, Dallas SL, Maser R, Calvet JP, Bonewald L. Cilia-like structures and polycystin-1 in osteoblasts/osteocytes and associated abnormalities in skeletogenesis and Runx2 expression. Journal of Biological Chemistry. 2006; 281(41):30884–30895. [PubMed: 16905538]
40. Uzbekov R, Maurel D, Aveline P, Pallu S, Benhamou C, Rochefort G. Centrosome Fine Ultrastructure of the Osteocyte Mechanosensitive Primary Cilium. Microscopy and Microanalysis. 2012; 18(6):1430. [PubMed: 23171702]
41. Federman M, Nichols G Jr. Bone cell cilia: vestigial or functional organelles? Calcif Tissue Res. 1974; 17(1):81–5. [PubMed: 4451879]
42. Temiyasathit S, Jacobs CR. Osteocyte primary cilium and its role in bone mechanotransduction. Ann N Y Acad Sci. 2010; 1192(1):422–428. [PubMed: 20392268]
43. Anderson CT, Castillo AB, Brugmann SA, Helms JA, Jacobs CR, Stearns T. Primary cilia: cellular sensors for the skeleton. Anat Rec (Hoboken). 2008; 291(9):1074–8. [PubMed: 18727074]
44. Whitfield J. The solitary (primary) cilium–a mechanosensory toggle switch in bone and cartilage cells. Cell Signal. 2008; 20(6):1019–1024. [PubMed: 18248958]
45. Hoey DA, Tormey S, Ramcharan S, O'Brien FJ, Jacobs CR. Primary Cilia-Mediated Mechanotransduction in Human Mesenchymal Stem Cells. Stem Cells. 2012; 30(11):2561–2570. [PubMed: 22969057]
46. Christensen ST, Pedersen LB, Schneider L, Satir P. Sensory cilia and integration of signal transduction in human health and disease. Traffic. 2007; 8(2):97–109. [PubMed: 17241444]
47. Wong SY, Reiter JF. The primary cilium: at the crossroads of mammalian hedgehog signaling. Curr Top Dev Biol. 2008; 85:225–260. [PubMed: 19147008]
48. Huangfu D, Anderson KV. Cilia and Hedgehog responsiveness in the mouse. Proc Natl Acad Sci U S A. 2005; 102(32):11325–11330. [PubMed: 16061793]
49. Lancaster MA, Gleeson JG. The primary cilium as a cellular signaling center: lessons from disease. Curr Opin Genet Dev. 2009; 19(3):220–229. [PubMed: 19477114]
50. Karp SJ, Schipani E, St-Jacques B, Hunzelman J, Kronenberg H, McMahon AP. Indian hedgehog coordinates endochondral bone growth and morphogenesis via parathyroid hormone related-protein-dependent and-independent pathways. Development. 2000; 127(3):543–548. [PubMed: 10631175]
51. St-Jacques B, Hammerschmidt M, McMahon AP. Indian hedgehog signaling regulates proliferation and differentiation of chondrocytes and is essential for bone formation. Genes Dev. 1999; 13(16):2072–2086. [PubMed: 10465785]
52. Pan A, Chang L, Nguyen A, James AW. A review of hedgehog signaling in cranial bone development. Frontiers in physiology. 2013; 4

53. Spinella-Jaegle S, Rawadi G, Kawai S, Gallea S, Faucheu C, Mollat P, Courtois B, Bergaud B, Ramez V, Blanchet AM. Sonic hedgehog increases the commitment of pluripotent mesenchymal cells into the osteoblastic lineage and abolishes adipocytic differentiation. J Cell Sci. 2001; 114(11):2085–2094. [PubMed: 11493644]
54. Drossopoulou G, Lewis K, Sanz-Ezquerro J, Nikbakht N, McMahon A, Hofmann C, Tickle C. A model for anteroposterior patterning of the vertebrate limb based on sequential long-and short-range Shh signalling and Bmp signalling. Development. 2000; 127(7):1337–1348. [PubMed: 10704381]
55. Litingtung Y, Dahn RD, Li Y, Fallon JF, Chiang C. Shh and Gli3 are dispensable for limb skeleton formation but regulate digit number and identity. Nature. 2002; 418(6901):979–983. [PubMed: 12198547]
56. Huangfu D, Liu A, Rakeman AS, Murcia NS, Niswander L, Anderson KV. Hedgehog signalling in the mouse requires intraflagellar transport proteins. Nature. 2003; 426(6962):83–87. [PubMed: 14603322]
57. Goetz SC, Ocbina PJ, Anderson KV. The primary cilium as a Hedgehog signal transduction machine. Methods in cell biology. 2009; 94:199–222. [PubMed: 20362092]
58. Tasouri E, Tucker KL. Primary cilia and organogenesis: is Hedgehog the only sculptor? Cell and tissue research. 2011; 345(1):21–40. [PubMed: 21638207]
59. Rohatgi R, Milenkovic L, Scott MP. Patched1 regulates hedgehog signaling at the primary cilium. Science. 2007; 317(5836):372–376. [PubMed: 17641202]
60. Corbit KC, Aanstad P, Singla V, Norman AR, Stainier DY, Reiter JF. Vertebrate Smoothened functions at the primary cilium. Nature. 2005; 437(7061):1018–1021. [PubMed: 16136078]
61. Robbins DJ, Fei DL, Riobo NA. The hedgehog signal transduction network. Sci Signal. 2012; 5(246):re6. [PubMed: 23074268]
62. Baron R, Kneissel M. WNT signaling in bone homeostasis and disease: from human mutations to treatments. Nat Med. 2013; 19(2):179–192. [PubMed: 23389618]
63. Regard JB, Zhong Z, Williams BO, Yang Y. Wnt signaling in bone development and disease: making stronger bone with Wnts. Cold Spring Harb Perspect Biol. 2012; 4(12)
64. May-Simera HL, Kelley MW. Cilia, Wnt signaling, and the cytoskeleton. Signal transduction. 2012; 11:19.
65. Sugimura R, Li L. Noncanonical Wnt signaling in vertebrate development, stem cells, and diseases. Birth Defects Research Part C: Embryo Today: Reviews. 2010; 90(4):243–256.
66. Wang C, Yuan X, Yang S. IFT80 is essential for chondrocyte differentiation by regulating Hedgehog and Wnt signaling pathways. Exp Cell Res. 2013; 319(5):623–632. [PubMed: 23333501]
67. Ocbina PJR, Tuson M, Anderson KV. Primary cilia are not required for normal canonical Wnt signaling in the mouse embryo. PLoS One. 2009; 4(8):e6839. [PubMed: 19718259]
68. Awan A, Bell AJ, Satir P. Kin5 knockdown in Tetrahymena thermophila using RNAi blocks cargo transport of Gef1. PloS one. 2009; 4(3):e4873. [PubMed: 19290045]
69. Lunt SC, Haynes T, Perkins BD. Zebrafish ift57, ift88, and ift172 intraflagellar transport mutants disrupt cilia but do not affect hedgehog signaling. Developmental Dynamics. 2009; 238(7):1744–1759. [PubMed: 19517571]
70. Rix S, Calmont A, Scambler PJ, Beales PL. An Ift80 mouse model of short rib polydactyly syndromes shows defects in hedgehog signalling without loss or malformation of cilia. Hum Mol Genet. 2011; 20(7):1306–1314. [PubMed: 21227999]
71. Vanhooren V, Libert C. The mouse as a model organism in aging research: Usefulness, pitfalls and possibilities. Ageing research reviews. 2013; 12(1):8–21. [PubMed: 22543101]
72. Elefteriou F, Yang X. Genetic mouse models for bone studies—Strengths and limitations. Bone. 2011; 49(6):1242–1254. [PubMed: 21907838]
73. Marshall WF. Basal bodies platforms for building cilia. Curr Top Dev Biol. 2008; 85:1–22. [PubMed: 19147000]
74. Ringo DL. Flagellar motion and fine structure of the flagellar apparatus in Chlamydomonas. The Journal of cell biology. 1967; 33(3):543–571. [PubMed: 5341020]

75. Satir P, Christensen ST. Overview of structure and function of mammalian cilia. Annu Rev Physiol. 2007; 69:377–400. [PubMed: 17009929]
76. Kozminski KG, Johnson KA, Forscher P, Rosenbaum JL. A motility in the eukaryotic flagellum unrelated to flagellar beating. Proc Natl Acad Sci U S A. 1993; 90(12):5519–23. [PubMed: 8516294]
77. Orozco JT, Wedaman KP, Signor D, Brown H, Rose L, Scholey JM. Movement of motor and cargo along cilia. Nature. 1999; 398(6729):674–674. [PubMed: 10227290]
78. Cole DG, Diener DR, Himelblau AL, Beech PL, Fuster JC, Rosenbaum JL. Chlamydomonas kinesin-II-dependent intraflagellar transport (IFT): IFT particles contain proteins required for ciliary assembly in Caenorhabditis elegans sensory neurons. J Cell Biol. 1998; 141(4):993–1008. [PubMed: 9585417]
79. Pazour GJ, Wilkerson CG, Witman GB. A dynein light chain is essential for the retrograde particle movement of intraflagellar transport (IFT). J Cell Biol. 1998; 141(4):979–92. [PubMed: 9585416]
80. Mizuno N, Taschner M, Engel BD, Lorentzen E. Structural studies of ciliary components. J Mol Biol. 2012; 422(2):163–80. [PubMed: 22683354]
81. Kozminski KG. Intraflagellar transport—the “new motility” 20 years later. Mol Biol Cell. 2012; 23(5):751–753. [PubMed: 22379118]
82. Cole DG, Diener DR, Himelblau AL, Beech PL, Fuster JC, Rosenbaum JL. Chlamydomonas kinesin-II–dependent intraflagellar transport (IFT): IFT particles contain proteins required for ciliary assembly in Caenorhabditis elegans sensory neurons. J Cell Biol. 1998; 141(4):993–1008. [PubMed: 9585417]
83. Piperno G, Mead K. Transport of a novel complex in the cytoplasmic matrix of Chlamydomonas flagella. Proceedings of the National Academy of Sciences. 1997; 94(9):4457–4462.
84. Cole, DG. The Chlamydomonas Sourcebook. Ed G. B. Witman; 2009. Intraflagellar transport.
85. Piperno G, Siuda E, Henderson S, Segil M, Vaananen H, Sassaroli M. Distinct mutants of retrograde intraflagellar transport (IFT) share similar morphological and molecular defects. J Cell Biol. 1998; 143(6):1591–1601. [PubMed: 9852153]
86. Pedersen LB, Rosenbaum JL. Intraflagellar transport (IFT) role in ciliary assembly, resorption and signalling. Curr Top Dev Biol. 2008; 85:23–61. [PubMed: 19147001]
87. Lucker BF, Behal RH, Qin H, Siron LC, Taggart WD, Rosenbaum JL, Cole DG. Characterization of the intraflagellar transport complex B core: direct interaction of the IFT81 and IFT74/72 subunits. J Biol Chem. 2005; 280(30):27688–96. [PubMed: 15955805]
88. Qin H, Diener DR, Geimer S, Cole DG, Rosenbaum JL. Intraflagellar transport (IFT) cargo IFT transports flagellar precursors to the tip and turnover products to the cell body. J Cell Biol. 2004; 164(2):255–266. [PubMed: 14718520]
89. Follit JA, Xu F, Keady BT, Pazour GJ. Characterization of mouse IFT complex B. Cell Motil Cytoskeleton. 2009; 66(8):457–468. [PubMed: 19253336]
90. Cole DG, Snell WJ. SnapShot: Intraflagellar transport. Cell. 2009; 137(4):784. [PubMed: 19450523]
91. Murcia NS, Richards WG, Yoder BK, Mucenski ML, Dunlap JR, Woychik RP. The Oak Ridge Polycystic Kidney (orpk) disease gene is required for left-right axis determination. Development. 2000; 127(11):2347–2355. [PubMed: 10804177]
92. Friedland-Little JM, Hoffmann AD, Ocbina PJ, Peterson MA, Bosman JD, Chen Y, Cheng SY, Anderson KV, Moskowitz IP. A novel murine allele of Intraflagellar Transport Protein 172 causes a syndrome including VACTERL-like features with hydrocephalus. Hum Mol Genet. 2011; 20(19):3725–37. [PubMed: 21653639]
93. Song B, Haycraft CJ, Seo H-s, Yoder BK, Serra R. Development of the post-natal growth plate requires intraflagellar transport proteins. Developmental biology. 2007; 305(1):202–216. [PubMed: 17359961]
94. Marszalek JR, Ruiz-Lozano P, Roberts E, Chien KR, Goldstein LS. Situs inversus and embryonic ciliary morphogenesis defects in mouse mutants lacking the KIF3A subunit of kinesin-II. Proceedings of the National Academy of Sciences. 1999; 96(9):5043–5048.
95. Stottmann RW, Tran PV, Turbe-Doan A, Beier DR. Ttc21b is required to restrict sonic hedgehog activity in the developing mouse forebrain. Dev Biol. 2009; 335(1):166–78. [PubMed: 19732765]

96. Tran PV, Haycraft CJ, Besschetnova TY, Turbe-Doan A, Stottmann RW, Herron BJ, Chesebro AL, Qiu H, Scherz PJ, Shah JV, Yoder BK, Beier DR. THM1 negatively modulates mouse sonic hedgehog signal transduction and affects retrograde intraflagellar transport in cilia. Nat Genet. 2008; 40(4):403–10. [PubMed: 18327258]

97. Cortellino S, Wang C, Wang B, Bassi MR, Caretti E, Champeval D, Calmont A, Jarnik M, Burch J, Zaret KS, Larue L, Bellacosa A. Defective ciliogenesis, embryonic lethality and severe impairment of the Sonic Hedgehog pathway caused by inactivation of the mouse complex A intraflagellar transport gene Ift122/Wdr10, partially overlapping with the DNA repair gene Med1/Mbd4. Dev Biol. 2009; 325(1):225–37. [PubMed: 19000668]

98. Nachury MV, Loktev AV, Zhang Q, Westlake CJ, Peränen J, Merdes A, Slusarski DC, Scheller RH, Bazan JF, Sheffield VC. A core complex of BBS proteins cooperates with the GTPase Rab8 to promote ciliary membrane biogenesis. Cell. 2007; 129(6):1201–1213. [PubMed: 17574030]

99. Loktev AV, Zhang Q, Beck JS, Searby CC, Scheetz TE, Bazan JF, Slusarski DC, Sheffield VC, Jackson PK, Nachury MV. A BBSome subunit links ciliogenesis, microtubule stability, and acetylation. Dev Cell. 2008; 15(6):854–65. [PubMed: 19081074]

100. Sung CH, Leroux MR. The roles of evolutionarily conserved functional modules in cilia-related trafficking. Nature cell biology. 2013; 15(12):1387–1397.

101. Ruiz-Perez VL, Blair HJ, Rodriguez-Andres ME, Blanco MJ, Wilson A, Liu YN, Miles C, Peters H, Goodship JA. Evc is a positive mediator of Ihh-regulated bone growth that localises at the base of chondrocyte cilia. Development. 2007; 134(16):2903–2912. [PubMed: 17660199]

102. Romio L, Wright V, Price K, Winyard PJ, Donnai D, Porteous ME, Franco B, Giorgio G, Malcolm S, Woolf AS, Feather SA. OFD1, the gene mutated in oral-facial-digital syndrome type 1, is expressed in the metanephros and in human embryonic renal mesenchymal cells. J Am Soc Nephrol. 2003; 14(3):680–9. [PubMed: 12595504]

103. Zimmermann KW. Beiträge zur Kenntniss einiger Drüsen und Epithelien. Archiv für mikroskopische Anatomie. 1898; 52(3):552–706.

104. Novarino G, Akizu N, Gleeson JG. Modeling human disease in humans: the ciliopathies. Cell. 2011; 147(1):70–79. [PubMed: 21962508]

105. Lee JE, Gleeson JG. A systems-biology approach to understanding the ciliopathy disorders. Genome Med. 2011; 3:59. [PubMed: 21943201]

106. Jeune M, Beraud C, Carron R. Asphyxiating thoracic dystrophy with familial characteristics. Arch Fr Pediatr. 1955; 12(8):886–91. [PubMed: 13292988]

107. De Vries J, Yntema J, Van Die C, Crama N, Cornelissen E, Hamel B. Jeune syndrome: description of 13 cases and a proposal for follow-up protocol. European journal of pediatrics. 2010; 169(1):77–88. [PubMed: 19430947]

108. Davis EE, Zhang Q, Liu Q, Diplas BH, Davey LM, Hartley J, Stoetzel C, Szymanska K, Ramaswami G, Logan CV, Muzny DM, Young AC, Wheeler DA, Cruz P, Morgan M, Lewis LR, Cherukuri P, Maskeri B, Hansen NF, Mullikin JC, Blakesley RW, Bouffard GG, Program NCS, Gyapay G, Rieger S, Tonshoff B, Kern I, Soliman NA, Neuhaus TJ, Swoboda KJ, Kayserili H, Gallagher TE, Lewis RA, Bergmann C, Otto EA, Saunier S, Scambler PJ, Beales PL, Gleeson JG, Maher ER, Attie-Bitach T, Dollfus H, Johnson CA, Green ED, Gibbs RA, Hildebrandt F, Pierce EA, Katsanis N. TTC21B contributes both causal and modifying alleles across the ciliopathy spectrum. Nat Genet. 2011; 43(3):189–96. [PubMed: 21258341]

109. Bredrup C, Saunier S, Oud MM, Fiskerstrand T, Hoischen A, Brackman D, Leh SM, Midtbo M, Filhol E, Bole-Feysot C, Nitschke P, Gilissen C, Haugen OH, Sanders JS, Stolte-Dijkstra I, Mans DA, Steenbergen EJ, Hamel BC, Matignon M, Pfundt R, Jeanpierre C, Boman H, Rodahl E, Veltman JA, Knappskog PM, Knoers NV, Roepman R, Arts HH. Ciliopathies with skeletal anomalies and renal insufficiency due to mutations in the IFT-A gene *WDR19*. Am J Hum Genet. 2011; 89(5):634–43. [PubMed: 22019273]

110. Baujat G, Huber C, El Hokayem J, Caumes R, Do Ngoc Thanh C, David A, Delezoide AL, Dieux-Coeslier A, Estournet B, Francannet C, Kayirangwa H, Lacaille F, Le Bourgeois M, Martinovic J, Salomon R, Sigaudy S, Malan V, Munnich A, Le Merrer M, Le Quan Sang KH, Cormier-Daire V. Asphyxiating thoracic dysplasia: clinical and molecular review of 39 families. J Med Genet. 2013; 50(2):91–8. [PubMed: 23339108]

111. Perrault I, Saunier S, Hanein S, Filhol E, Bizet AA, Collins F, Salih MA, Gerber S, Delphin N, Bigot K, Orssaud C, Silva E, Baudouin V, Oud MM, Shannon N, Le Merrer M, Roche O, Pietrement C, Goumid J, Baumann C, Bole-Feysot C, Nitschke P, Zahrate M, Beales P, Arts HH, Munnich A, Kaplan J, Antignac C, Cormier-Daire V, Rozet JM. Mainzer-Saldino syndrome is a ciliopathy caused by IFT140 mutations. Am J Hum Genet. 2012; 90(5):864–70. [PubMed: 22503633]

112. Schmidts M, Frank V, Eisenberger T, al Turki S, Bizet AA, Antony D, Rix S, Decker C, Bachmann N, Bald M. Combined NGS approaches identify mutations in the intraflagellar transport gene IFT140 in skeletal ciliopathies with early progressive kidney disease. Human mutation. 2013; 34(5):714–724. [PubMed: 23418020]

113. Forsythe E, Beales PL. Bardet–Biedl syndrome. European Journal of Human Genetics. 2012; 21(1):8–13. [PubMed: 22713813]

114. Karmous-Benailly H, Martinovic J, Gubler MC, Sirot Y, Clech L, Ozilou C, Augé J, Brahimi N, Etchevers H, Detrait E. Antenatal presentation of Bardet-Biedl syndrome may mimic Meckel syndrome. Am J Hum Genet. 2005; 76(3):493. [PubMed: 15666242]

115. Ellis RW, Van Creveld S. A Syndrome Characterized by Ectodermal Dysplasia, Polydactyly, Chondro-Dysplasia and Congenital Morbus Cordis Report of Three Cases. Arch Dis Child. 1940; 15(82):65–84. [PubMed: 21032169]

116. Ruiz-Perez, VL.; Goodship, JA. American Journal of Medical Genetics Part C: Seminars in Medical Genetics. Wiley Online Library; 2009. Ellis–van Creveld syndrome and Weyers acrodental dysostosis are caused by cilia-mediated diminished response to hedgehog ligands.

117. D'Asdia MC, Torrente I, Consoli F, Ferese R, Magliozzi M, Bernardini L, Guida V, Digilio MC, Marino B, Dallapiccola B, De Luca A. Novel and recurrent EVC and EVC2 mutations in Ellis-van Creveld syndrome and Weyers acrofacial dyostosis. European journal of medical genetics. 2013; 56(2):80–7. [PubMed: 23220543]

118. Ruiz-Perez VL, Ide SE, Strom TM, Lorenz B, Wilson D, Woods K, King L, Francomano C, Freisinger P, Spranger S, Marino B, Dallapiccola B, Wright M, Meitinger T, Polymeropoulos MH, Goodship J. Mutations in a new gene in Ellis-van Creveld syndrome and Weyers acrodental dysostosis. Nat Genet. 2000; 24(3):283–6. [PubMed: 10700184]

119. Ruiz-Perez VL, Tompson W Stuart, Blair J Helen, Espinoza-Valdez C, Lapunzina P, Silva EO, Hamel B, Gibbs JL, Young ID, Wright MJ. Mutations in two nonhomologous genes in a head-to-head configuration cause Ellis-van Creveld syndrome. The American Journal of Human Genetics. 2003; 72(3):728–732.

120. Tompson SW, Ruiz-Perez VL, Blair HJ, Barton S, Navarro V, Robson JL, Wright MJ, Goodship JA. Sequencing EVC and EVC2 identifies mutations in two-thirds of Ellis–van Creveld syndrome patients. Hum Genet. 2007; 120(5):663–670. [PubMed: 17024374]

121. Valencia M, Lapunzina P, Lim D, Zannolli R, Bartholdi D, Wollnik B, Al-Ajlouni O, Eid SS, Cox H, Buoni S. Widening the mutation spectrum of EVC and EVC2: ectopic expression of Weyer variants in NIH 3T3 fibroblasts disrupts Hedgehog signaling. Hum Mutat. 2009; 30(12): 1667–1675. [PubMed: 19810119]

122. Naiboglu B, Oysu C, Gokceer T. Orofaciodigital syndrome. Ear, nose, & throat journal. 2012; 91(1):E8.

123. Gurrieri F, Franco B, Toriello H, Neri G. Oral–facial–digital syndromes: review and diagnostic guidelines. American Journal of Medical Genetics Part A. 2007; 143(24):3314–3323. [PubMed: 17963220]

124. Baraitser M. The orofaciodigital (OFD) syndromes. Journal of medical genetics. 1986; 23(2):116. [PubMed: 3712388]

125. Burn J, Dezateux C, Hall C, Baraitser M. Orofaciodigital syndrome with mesomelic limb shortening. Journal of medical genetics. 1984; 21(3):189–192. [PubMed: 6748015]

126. Ferrante MI, Feather SA, Bulfone A, Wright V, Ghiani M, Selicorni A, Gammaro L, Scolari F, Woolf AS, Sylvie O. Identification of the gene for oral-facial-digital type I syndrome. The American Journal of Human Genetics. 2001; 68(3):569–576.

127. Romio L, Fry AM, Winyard PJ, Malcolm S, Woolf AS, Feather SA. OFD1 is a centrosomal/basal body protein expressed during mesenchymal-epithelial transition in human nephrogenesis. Journal of the American Society of Nephrology. 2004; 15(10):2556–2568. [PubMed: 15466260]

128. Thiel C, Kessler K, Giessl A, Dimmler A, Shalev SA, von der Haar S, Zenker M, Zahnleiter D, Stöss H, Beinder E. *NEK1* Mutations Cause Short-Rib Polydactyly Syndrome Type Majewski. The American Journal of Human Genetics. 2011; 88(1):106–114.

129. Ho NC, Francomano CA, van Allen M. Jeune asphyxiating thoracic dystrophy and short-rib polydactyly type III (Verma-Naumoff) are variants of the same disorder. Am J Med Genet. 2000; 90(4):310–314. [PubMed: 10710229]

130. Cavalcanti DP, Huber C, Sang KHLQ, Baujat G, Collins F, Delezoide AL, Dagoneau N, Le Merrer M, Martinovic J, Mello MFS. Mutation in IFT80 in a fetus with the phenotype of Verma-Naumoff provides molecular evidence for Jeune-Verma-Naumoff dysplasia spectrum. J Med Genet. 2011; 48(2):88–92. [PubMed: 19648123]

131. El Hokayem J, Huber C, Couvé A, Aziza J, Baujat G, Bouvier R, Cavalcanti DP, Collins FA, Cordier M-P, Delezoide A-L. NEK1 and DYNC2H1 are both involved in short rib polydactyly Majewski type but not in Beemer Langer cases. J Med Genet. 2012; 49(4):227–233. [PubMed: 22499340]

132. Walczak-Sztulpa J, Eggenschwiler J, Osborn D, Brown DA, Emma F, Klingenberg C, Hennekam RC, Torre G, Garshasbi M, Tzschach A. Cranioectodermal Dysplasia, Sensenbrenner Syndrome, Is a Ciliopathy Caused by Mutations in the *IFT122* Gene. The American Journal of Human Genetics. 2010; 86(6):949–956.

133. Konstantinidou AE, Fryssira H, Sifakis S, Karadimas C, Kaminopetros P, Agrogiannis G, Velonis S, Nikkels PG, Patsouris E. Cranioectodermal dysplasia: a probable ciliopathy. American Journal of Medical Genetics Part A. 2009; 149(10):2206–2211. [PubMed: 19760621]

134. Levin LS, Perrin J, Ose L, Dorst JP, Miller JD, McKusick VA. A heritable syndrome of craniosynostosis, short thin hair, dental abnormalities, and short limbs: cranioectodermal dysplasia. J Pediatr. 1977; 90(1):55–61. [PubMed: 830894]

135. Arts HH, Bongers EM, Mans DA, van Beersum SE, Oud MM, Bolat E, Spruijt L, Cornelissen EA, Schuurs-Hoeijmakers JH, de Leeuw N. C14ORF179 encoding IFT43 is mutated in Sensenbrenner syndrome. J Med Genet. 2011; 48(6):390–395. [PubMed: 21378380]

136. Gilissen C, Arts HH, Hoischen A, Spruijt L, Mans DA, Arts P, van Lier B, Steehouwer M, van Reeuwijk J, Kant SG, Roepman R, Knoers NV, Veltman JA, Brunner HG. Exome sequencing identifies WDR35 variants involved in Sensenbrenner syndrome. Am J Hum Genet. 2010; 87(3): 418–23. [PubMed: 20817137]

137. Hoffer JL, Fryssira H, Konstantinidou AE, Ropers HH, Tzschach A. Novel WDR35 mutations in patients with cranioectodermal dysplasia (Sensenbrenner syndrome). Clin Genet. 2013; 83(1): 92–5. [PubMed: 22486404]

138. Chen CP. Meckel syndrome: genetics, perinatal findings, and differential diagnosis. Taiwanese Journal of Obstetrics and Gynecology. 2007; 46(1):9–14. [PubMed: 17389183]

139. Delous M, Baala L, Salomon R, Laclef C, Vierkotten J, Tory K, Golzio C, Lacoste T, Besse L, Ozilou C. The ciliary gene RPGRIP1L is mutated in cerebello-oculo-renal syndrome (Joubert syndrome type B) and Meckel syndrome. Nat Genet. 2007; 39(7):875–881. [PubMed: 17558409]

140. Roume J, Genin E, Cormier-Daire V, Ma H, Mehaye B, Attie T, Razavi-Encha F, Fallet-Bianco C, Buenerd A, Clerget-Darpoux F. A gene for Meckel syndrome maps to chromosome 11q13. The American Journal of Human Genetics. 1998; 63(4):1095–1101.

141. Leightner AC, Hommerding CJ, Peng Y, Salisbury JL, Gainullin VG, Czarnecki PG, Sussman CR, Harris PC. The Meckel syndrome protein meckelin (TMEM67) is a key regulator of cilia function but is not required for tissue planar polarity. Hum Mol Genet. 2013

142. Kyttälä M, Tallila J, Salonen R, Kopra O, Kohlschmidt N, Paavola-Sakki P, Peltonen L, Kestilä M. MKS1, encoding a component of the flagellar apparatus basal body proteome, is mutated in Meckel syndrome. Nat Genet. 2006; 38(2):155–157. [PubMed: 16415886]

143. Smith UM, Consugar M, Tee LJ, McKee BM, Maina EN, Whelan S, Morgan NV, Goranson E, Gissen P, Lilliquist S, Aligianis IA, Ward CJ, Pasha S, Punyashthiti R, Sharif S Malik, Batman PA, Bennett CP, Woods CG, McKeown C, Bucourt M, Miller CA, Cox P, Algazali L, Trembath

RC, Torres VE, Attie-Bitach T, Kelly DA, Maher ER, Gattone VH 2nd, Harris PC, Johnson CA. The transmembrane protein meckelin (MKS3) is mutated in Meckel-Gruber syndrome and the wpk rat. Nat Genet. 2006; 38(2):191–6. [PubMed: 16415887]

144. Szymanska K, Berry I, Logan CV, Cousins SR, Lindsay H, Jafri H, Raashid Y, Malik-Sharif S, Castle B, Ahmed M. Founder mutations and genotype-phenotype correlations in Meckel-Gruber syndrome and associated ciliopathies. Cilia. 2012; 1(1):18. [PubMed: 23351400]
145. Hardouin SN, Nagy A. Mouse models for human disease. Clinical genetics. 2000; 57(4):237–244. [PubMed: 10845564]
146. Hofker, MH.; van Deursen, JM. Transgenic mouse: methods and protocols. Springer; 2002.
147. Thomas KR, Capecchi MR. Site-directed mutagenesis by gene targeting in mouse embryo-derived stem cells. Cell. 1987; 51(3):503–512. [PubMed: 2822260]
148. Kühn, R.; Torres, RM. Transgenesis Techniques. Springer; 2002. Cre/loxP recombination system and gene targeting.
149. Nagy A. Cre recombinase: the universal reagent for genome tailoring. Genesis. 2000; 26(2):99–109. [PubMed: 10686599]
150. VanKoevering KK, Williams BO. Transgenic mouse strains for conditional gene deletion during skeletal development. IBMS BoneKEy. 2008; 5(5):151–170.
151. Loonstra A, Vooijs M, Beverloo HB, Al Allak B, van Drunen E, Kanaar R, Berns A, Jonkers J. Growth inhibition and DNA damage induced by Cre recombinase in mammalian cells. Proceedings of the National Academy of Sciences. 2001; 98(16):9209–9214.
152. Russell W, Kelly E, Hunsicker P, Bangham J, Maddux S, Phipps E. Specific-locus test shows ethylnitrosourea to be the most potent mutagen in the mouse. Proceedings of the National Academy of Sciences. 1979; 76(11):5818–5819.
153. Stanford WL, Cohn JB, Cordes SP. Gene-trap mutagenesis: past, present and beyond. Nature reviews genetics. 2001; 2(10):756–768.
154. De-Zolt, S.; Altschmied, J.; Ruiz, P.; von Melchner, H.; Schnütgen, F. Gene Knockout Protocols. Springer; 2009. Gene-trap vectors and mutagenesis.
155. Gross C, De Baere E, Lo A, Chang W, Messiaen L. Cloning and characterization of human WDR10, a novel gene located at 3q21 encoding a WD-repeat protein that is highly expressed in pituitary and testis. DNA and cell biology. 2001; 20(1):41–52. [PubMed: 11242542]
156. Qin J, Lin Y, Norman RX, Ko HW, Eggenschwiler JT. Intraflagellar transport protein 122 antagonizes Sonic Hedgehog signaling and controls ciliary localization of pathway components. Proc Natl Acad Sci U S A. 2011; 108(4):1456–61. [PubMed: 21209331]
157. Cortellino S, Turner D, Masciullo V, Schepis F, Albino D, Daniel R, Skalka AM, Meropol NJ, Alberti C, Larue L. The base excision repair enzyme MED1 mediates DNA damage response to antitumor drugs and is associated with mismatch repair system integrity. Proceedings of the National Academy of Sciences. 2003; 100(25):15071–15076.
158. Qin J, Lin Y, Norman RX, Ko HW, Eggenschwiler JT. Intraflagellar transport protein 122 antagonizes Sonic Hedgehog signaling and controls ciliary localization of pathway components. Proceedings of the National Academy of Sciences. 2011; 108(4):1456–1461.
159. Efimenko E, Blacque OE, Ou G, Haycraft CJ, Yoder BK, Scholey JM, Leroux MR, Swoboda P. Caenorhabditis elegans DYF-2, an orthologue of human WDR19, is a component of the intraflagellar transport machinery in sensory cilia. Mol Biol Cell. 2006; 17(11):4801–11. [PubMed: 16957054]
160. Ashe A, Butterfield NC, Town L, Courtney AD, Cooper AN, Ferguson C, Barry R, Olsson F, Liem KF Jr, Parton RG, Wainwright BJ, Anderson KV, Whitelaw E, Wicking C. Mutations in mouse Ift144 model the craniofacial, limb and rib defects in skeletal ciliopathies. Hum Mol Genet. 2012; 21(8):1808–23. [PubMed: 22228095]
161. Liem KF, Ashe A, He M, Satir P, Moran J, Beier D, Wicking C, Anderson KV. The IFT-A complex regulates Shh signaling through cilia structure and membrane protein trafficking. The Journal of cell biology. 2012; 197(6):789–800. [PubMed: 22689656]
162. Jonassen JA, SanAgustin J, Baker SP, Pazour GJ. Disruption of IFT complex A causes cystic kidneys without mitotic spindle misorientation. Journal of the American Society of Nephrology. 2012; 23(4):641–651. [PubMed: 22282595]

163. Caruana G, Farlie PG, Hart AH, Bagheri-Fam S, Wallace MJ, Dobbie MS, Gordon CT, Miller KA, Whittle B, Abud HE, Arkell RM, Cole TJ, Harley VR, Smyth IM, Bertram JF. Genome-wide ENU mutagenesis in combination with high density SNP analysis and exome sequencing provides rapid identification of novel mouse models of developmental disease. PLoS One. 2013; 8(3):e55429. [PubMed: 23469164]
164. Miller KA, Ah-Cann CJ, Welfare MF, Tan TY, Pope K, Caruana G, Freckmann ML, Savarirayan R, Bertram JF, Dobbie MS. Cauli: A Mouse Strain with an Ift140 Mutation That Results in a Skeletal Ciliopathy Modelling Jeune Syndrome. PLoS Genet. 2013; 9(8):e1003746. [PubMed: 24009529]
165. Follit JA, Tuft RA, Fogarty KE, Pazour GJ. The intraflagellar transport protein IFT20 is associated with the Golgi complex and is required for cilia assembly. Molecular biology of the cell. 2006; 17(9):3781–3792. [PubMed: 16775004]
166. Follit JA, San Agustin JT, Xu F, Jonassen JA, Samtani R, Lo CW, Pazour GJ. The Golgin GMAP210/TRIP11 anchors IFT20 to the Golgi complex. PLoS genetics. 2008; 4(12):e1000315. [PubMed: 19112494]
167. Finetti F, Paccani SR, Riparbelli MG, Giacomello E, Perinetti G, Pazour GJ, Rosenbaum JL, Baldari CT. Intraflagellar transport is required for polarized recycling of the TCR/CD3 complex to the immune synapse. Nature cell biology. 2009; 11(11):1332–1339.
168. Moyer JH, Lee-Tischler MJ, Kwon HY, Schrick JJ, Avner ED, Sweeney WE, Godfrey VL, Cacheiro N, Wilkinson J, Woychik RP. Candidate gene associated with a mutation causing recessive polycystic kidney disease in mice. Science. 1994; 264(5163):1329–1333. [PubMed: 8191288]
169. Lehman JM, Michaud EJ, Schoeb TR, Aydin-Son Y, Miller M, Yoder BK. The Oak Ridge Polycystic Kidney mouse: modeling ciliopathies of mice and men. Developmental Dynamics. 2008; 237(8):1960–1971. [PubMed: 18366137]
170. Zhang Q, Murcia NS, Chittenden LR, Richards WG, Michaud EJ, Woychik RP, Yoder BK. Loss of the Tg737 protein results in skeletal patterning defects. Developmental Dynamics. 2003; 227(1):78–90. [PubMed: 12701101]
171. McGlashan S, Haycraft C, Jensen C, Yoder B, Poole C. Articular cartilage and growth plate defects are associated with chondrocyte cytoskeletal abnormalities in Tg737orpk mice lacking the primary cilia protein polaris. Matrix biology: journal of the International Society for Matrix Biology. 2007; 26(4):234. [PubMed: 17289363]
172. Irianto J, Ramaswamy G, Serra R, Knight MM. Depletion of primary cilia reduces the compressive modulus of articular cartilage. J Biomech. 2013
173. Liu A, Wang B, Niswander LA. Mouse intraflagellar transport proteins regulate both the activator and repressor functions of Gli transcription factors. Development. 2005; 132(13):3103–3111. [PubMed: 15930098]
174. Haycraft CJ, Zhang Q, Song B, Jackson WS, Detloff PJ, Serra R, Yoder BK. Intraflagellar transport is essential for endochondral bone formation. Development. 2007; 134(2):307–316. [PubMed: 17166921]
175. Chang CF, Serra R. Ift88 regulates Hedgehog signaling, Sfrp5 expression, and beta-catenin activity in post-natal growth plate. J Orthop Res. 2013; 31(3):350–6. [PubMed: 23034798]
176. Chang CF, Ramaswamy G, Serra R. Depletion of primary cilia in articular chondrocytes results in reduced Gli3 repressor to activator ratio, increased Hedgehog signaling, and symptoms of early osteoarthritis. Osteoarthritis and Cartilage. 2012; 20(2):152–161. [PubMed: 22173325]
177. Goodrich LV, Milenković L, Higgins KM, Scott MP. Altered neural cell fates and medulloblastoma in mouse patched mutants. Science. 1997; 277(5329):1109–1113. [PubMed: 9262482]
178. Ocbina PJ, Tuson M, Anderson KV. Primary cilia are not required for normal canonical Wnt signaling in the mouse embryo. PLoS One. 2009; 4(8):e6839. [PubMed: 19718259]
179. Gorivodsky M, Mukhopadhyay M, Wilsch-Braeuninger M, Phillips M, Teufel A, Kim C, Malik N, Huttner W, Westphal H. Intraflagellar transport protein 172 is essential for primary cilia formation and plays a vital role in patterning the mammalian brain. Dev Biol. 2009; 325(1):24–32. [PubMed: 18930042]

180. Howard PW, Howard TL, Maurer RA. Generation of mice with a conditional allele for Ift172. Transgenic research. 2010; 19(1):121–126. [PubMed: 19521792]

181. Baker SA, Freeman K, Luby-Phelps K, Pazour GJ, Besharse JC. IFT20 links kinesin II with a mammalian intraflagellar transport complex that is conserved in motile flagella and sensory cilia. Journal of Biological Chemistry. 2003; 278(36):34211–34218. [PubMed: 12821668]

182. Krock BL, Perkins BD. The intraflagellar transport protein IFT57 is required for cilia maintenance and regulates IFT-particle–kinesin-II dissociation in vertebrate photoreceptors. J Cell Sci. 2008; 121(11):1907–1915. [PubMed: 18492793]

183. Jonassen JA, San Agustin J, Follit JA, Pazour GJ. Deletion of IFT20 in the mouse kidney causes misorientation of the mitotic spindle and cystic kidney disease. The Journal of cell biology. 2008; 183(3):377–384. [PubMed: 18981227]

184. Keady BT, Le YZ, Pazour GJ. IFT20 is required for opsin trafficking and photoreceptor outer segment development. Molecular biology of the cell. 2011; 22(7):921–930. [PubMed: 21307337]

185. Keady BT, Samtani R, Tobita K, Tsuchya M, San Agustin JT, Follit JA, Jonassen JA, Subramanian R, Lo CW, Pazour GJ. IFT25 links the signal-dependent movement of hedgehog components to intraflagellar transport. Developmental cell. 2012; 22(5):940–951. [PubMed: 22595669]

186. Bhogaraju S, Taschner M, Morawetz M, Basquin C, Lorentzen E. Crystal structure of the intraflagellar transport complex 25/27. EMBO J. 2011; 30(10):1907–1918. [PubMed: 21505417]

187. Qin H, Wang Z, Diener D, Rosenbaum J. Intraflagellar transport protein 27 is a small G protein involved in cell-cycle control. Curr Biol. 2007; 17(3):193–202. [PubMed: 17276912]

188. Wang Z, Fan ZC, Williamson SM, Qin H. Intraflagellar transport (IFT) protein IFT25 is a phosphoprotein component of IFT complex B and physically interacts with IFT27 in Chlamydomonas. PLoS One. 2009; 4(5):e5384. [PubMed: 19412537]

189. Schafer JC, Winkelbauer ME, Williams CL, Haycraft CJ, Desmond RA, Yoder BK. IFTA-2 is a conserved cilia protein involved in pathways regulating longevity and dauer formation in Caenorhabditis elegans. J Cell Sci. 2006; 119(Pt 19):4088–100. [PubMed: 16968739]

190. Adhiambo C, Blisnick T, Toutirais G, Delannoy E, Bastin P. A novel function for the atypical small G protein Rab-like 5 in the assembly of the trypanosome flagellum. J Cell Sci. 2009; 122(6):834–841. [PubMed: 19240117]

191. Hou Y, Qin H, Follit JA, Pazour GJ, Rosenbaum JL, Witman GB. Functional analysis of an individual IFT protein: IFT46 is required for transport of outer dynein arms into flagella. J Cell Biol. 2007; 176(5):653–665. [PubMed: 17312020]

192. Gouttenoire J, Valcourt U, Bougault C, Aubert-Foucher E, Arnaud E, Giraud L, Mallein-Gerin F. Knockdown of the intraflagellar transport protein IFT46 stimulates selective gene expression in mouse chondrocytes and affects early development in zebrafish. Journal of Biological Chemistry. 2007; 282(42):30960–30973. [PubMed: 17720815]

193. Berbari NF, Kin NW, Sharma N, Michaud EJ, Kesterson RA, Yoder BK. Mutations in Traf3ip1 reveal defects in ciliogenesis, embryonic development, and altered cell size regulation. Dev Biol. 2011; 360(1):66–76. [PubMed: 21945076]

194. Niu Y, Murata T, Watanabe K, Kawakami K, Yoshimura A, Inoue J, Puri RK, Kobayashi N. MIP-T3 associates with IL-13Ralpha1 and suppresses STAT6 activation in response to IL-13 stimulation. FEBS Lett. 2003; 550(1–3):139–43. [PubMed: 12935900]

195. Gervais FG, Singaraja R, Xanthoudakis S, Gutekunst CA, Leavitt BR, Metzler M, Hackam AS, Tam J, Vaillancourt JP, Houtzager V. Recruitment and activation of caspase-8 by the Huntingtin-interacting protein Hip-1 and a novel partner Hippi. Nature cell biology. 2002; 4(2):95–105.

196. Houde C, Dickinson RJ, Houtzager VM, Cullum R, Montpetit R, Metzler M, Simpson EM, Roy S, Hayden MR, Hoodless PA. Hippi is essential for node cilia assembly and Sonic hedgehog signaling. Developmental biology. 2006; 300(2):523–533. [PubMed: 17027958]

197. Pathak N, Austin CA, Drummond IA. Tubulin tyrosine ligase-like genes ttll3 and ttll6 maintain zebrafish cilia structure and motility. Journal of Biological Chemistry. 2011; 286(13):11685–11695. [PubMed: 21262966]

198. Pathak N, Obara T, Mangos S, Liu Y, Drummond IA. The zebrafish fleer gene encodes an essential regulator of cilia tubulin polyglutamylation. Molecular biology of the cell. 2007; 18(11):4353–4364. [PubMed: 17761526]

199. Ou G, Blacque OE, Snow JJ, Leroux MR, Scholey JM. Functional coordination of intraflagellar transport motors. Nature. 2005; 436(7050):583–587. [PubMed: 16049494]

200. Bhogaraju S, Cajanek L, Fort C, Blisnick T, Weber K, Taschner M, Mizuno N, Lamla S, Bastin P, Nigg EA. Molecular Basis of Tubulin Transport Within the Cilium by IFT74 and IFT81. Science. 2013; 341(6149):1009–1012. [PubMed: 23990561]

201. Scholey JM. Intraflagellar transport motors in cilia: moving along the cell's antenna. J Cell Biol. 2008; 180(1):23–29. [PubMed: 18180368]

202. Rajagopalan V, D'Amico JP, Wilkes DE. Cytoplasmic dynein-2: from molecules to human diseases. Frontiers in Biology. 2013; 8(1):119–126.

203. Pfister KK, Fisher EM, Gibbons IR, Hays TS, Holzbaur EL, McIntosh JR, Porter ME, Schroer TA, Vaughan KT, Witman GB. Cytoplasmic dynein nomenclature. J Cell Biol. 2005; 171(3): 411–413. [PubMed: 16260502]

204. Ocbina PJR, Eggenschwiler JT, Moskowitz I, Anderson KV. Complex interactions between genes controlling trafficking in primary cilia. Nat Genet. 2011; 43(6):547–553. [PubMed: 21552265]

205. Ocbina PJR, Anderson KV. Intraflagellar transport, cilia, and mammalian Hedgehog signaling: analysis in mouse embryonic fibroblasts. Developmental Dynamics. 2008; 237(8):2030–2038. [PubMed: 18488998]

206. Liem KF, He M, Ocbina PJR, Anderson KV. Mouse Kif7/Costal2 is a cilia-associated protein that regulates Sonic hedgehog signaling. Proceedings of the National Academy of Sciences. 2009; 106(32):13377–13382.

207. May SR, Ashique AM, Karlen M, Wang B, Shen Y, Zarbalis K, Reiter J, Ericson J, Peterson AS. Loss of the retrograde motor for IFT disrupts localization of Smo to cilia and prevents the expression of both activator and repressor functions of Gli. Dev Biol. 2005; 287(2):378. [PubMed: 16229832]

208. Grissom PM, Vaisberg EA, McIntosh JR. Identification of a novel light intermediate chain (D2LIC) for mammalian cytoplasmic dynein 2. Mol Biol Cell. 2002; 13(3):817–829. [PubMed: 11907264]

209. Perrone CA, Tritschler D, Taulman P, Bower R, Yoder BK, Porter ME. A novel dynein light intermediate chain colocalizes with the retrograde motor for intraflagellar transport at sites of axoneme assembly in Chlamydomonas and mammalian cells. Mol Biol Cell. 2003; 14(5):2041–2056. [PubMed: 12802074]

210. Rana AA, Barbera JPM, Rodriguez TA, Lynch D, Hirst E, Smith JC, Beddington RS. Targeted deletion of the novel cytoplasmic dynein mD2LIC disrupts the embryonic organiser, formation of the body axes and specification of ventral cell fates. Development. 2004; 131(20):4999–5007. [PubMed: 15371312]

211. Verhey KJ, Dishinger J, Kee HL. Kinesin motors and primary cilia. Biochem Soc Trans. 2011; 39(5):1120. [PubMed: 21936775]

212. Scholey JM. Kinesin-2: A Family of Heterotrimeric and Homodimeric Motors with Diverse Intracellular Transport Functions. Annu Rev Cell Dev Biol. 2013; 29(1)

213. Miki H, Okada Y, Hirokawa N. Analysis of the kinesin superfamily: insights into structure and function. Trends Cell Biol. 2005; 15(9):467–76. [PubMed: 16084724]

214. Jenkins PM, Hurd TW, Zhang L, McEwen DP, Brown RL, Margolis B, Verhey KJ, Martens JR. Ciliary targeting of olfactory CNG channels requires the CNGB1b subunit and the kinesin-2 motor protein, KIF17. Current biology. 2006; 16(12):1211–1216. [PubMed: 16782012]

215. Cheung HO-L, Zhang X, Ribeiro A, Mo R, Makino S, Puviindran V, Law KK, Briscoe J, Hui C-c. The kinesin protein Kif7 is a critical regulator of Gli transcription factors in mammalian hedgehog signaling. Sci Signal. 2009; 2(76):ra29. [PubMed: 19549984]

216. Endoh-Yamagami S, Evangelista M, Wilson D, Wen X, Theunissen JW, Phamluong K, Davis M, Scales SJ, Solloway MJ, de Sauvage FJ. The mammalian Cos2 homolog Kif7 plays an essential role in modulating Hh signal transduction during development. Current biology. 2009; 19(15): 1320–1326. [PubMed: 19592253]

217. Marszalek JR, Liu X, Roberts EA, Chui D, Marth JD, Williams DS, Goldstein LS. Genetic evidence for selective transport of opsin and arrestin by kinesin-II in mammalian photoreceptors. Cell. 2000; 102(2):175–187. [PubMed: 10943838]

218. Kolpakova-Hart E, Jinnin M, Hou B, Fukai N, Olsen BR. Kinesin-2 controls development and patterning of the vertebrate skeleton by Hedgehog-and Gli3-dependent mechanisms. Dev Biol. 2007; 309(2):273–284. [PubMed: 17698054]

219. Brugmann SA, Allen NC, James AW, Mekonnen Z, Madan E, Helms JA. A primary cilia-dependent etiology for midline facial disorders. Hum Mol Genet. 2010; 19(8):1577–1592. [PubMed: 20106874]

220. Koyama E, Young B, Nagayama M, Shibukawa Y, Enomoto-Iwamoto M, Iwamoto M, Maeda Y, Lanske B, Song B, Serra R. Conditional Kif3a ablation causes abnormal hedgehog signaling topography, growth plate dysfunction, and excessive bone and cartilage formation during mouse skeletogenesis. Development. 2007; 134(11):2159–2169. [PubMed: 17507416]

221. Qiu N, Xiao Z, Cao L, Buechel MM, David V, Roan E, Quarles LD. Disruption of Kif3a in osteoblasts results in defective bone formation and osteopenia. J Cell Sci. 2012; 125(8):1945–1957. [PubMed: 22357948]

222. Temiyasathit S, Jacobs CR. Osteocyte primary cilium and its role in bone mechanotransduction. Annals of the New York Academy of Sciences. 2010; 1192(1):422–428. [PubMed: 20392268]

223. Kinumatsu T, Shibukawa Y, Yasuda T, Nagayama M, Yamada S, Serra R, Pacifici M, Koyama E. TMJ development and growth require primary cilia function. Journal of dental research. 2011; 90(8):988–994. [PubMed: 21566205]

224. Wu Y, Dai XQ, Li Q, Chen CX, Mai W, Hussain Z, Long W, Montalbetti N, Li G, Glynne R. Kinesin-2 mediates physical and functional interactions between polycystin-2 and fibrocystin. Hum Mol Genet. 2006; 15(22):3280–3292. [PubMed: 17008358]

225. Nonaka S, Tanaka Y, Okada Y, Takeda S, Harada A, Kanai Y, Kido M, Hirokawa N. Randomization of left–right asymmetry due to loss of nodal cilia generating leftward flow of extraembryonic fluid in mice lacking KIF3B motor protein. Cell. 1998; 95(6):829–837. [PubMed: 9865700]

226. Lum L, Beachy PA. The Hedgehog response network: sensors, switches, and routers. Science. 2004; 304(5678):1755–1759. [PubMed: 15205520]

227. Miki H, Okada Y, Hirokawa N. Analysis of the kinesin superfamily: insights into structure and function. Trends Cell Biol. 2005; 15(9):467–476. [PubMed: 16084724]

228. Tay SY, Ingham PW, Roy S. A homologue of the Drosophila kinesin-like protein Costal2 regulates Hedgehog signal transduction in the vertebrate embryo. Development. 2005; 132(4): 625–634. [PubMed: 15647323]

229. Wong-Riley MT, Besharse JC. The kinesin superfamily protein KIF17: one protein with many functions (. 2012

230. Howard PW, Jue SF, Maurer RA. Interaction of mouse TTC30/DYF-1 with multiple intraflagellar transport complex B proteins and KIF17. Exp Cell Res. 2013

231. Yin X, Takei Y, Kido MA, Hirokawa N. Molecular motor KIF17 is fundamental for memory and learning via differential support of synaptic NR2A/2B levels. Neuron. 2011; 70(2):310–325. [PubMed: 21521616]

232. Kim J, Lee JE, Heynen-Genel S, Suyama E, Ono K, Lee K, Ideker T, Aza-Blanc P, Gleeson JG. Functional genomic screen for modulators of ciliogenesis and cilium length. Nature. 2010; 464(7291):1048–1051. [PubMed: 20393563]

233. Beales PL, Bland E, Tobin JL, Bacchelli C, Tuysuz B, Hill J, Rix S, Pearson CG, Kai M, Hartley J. IFT80, which encodes a conserved intraflagellar transport protein, is mutated in Jeune asphyxiating thoracic dystrophy. Nat Genet. 2007; 39(6):727–729. [PubMed: 17468754]

234. Hao L, Scholey JM. Intraflagellar transport at a glance. Journal of cell science. 2009; 122(7):889–892. [PubMed: 19295122]

235. Arts HH, Knoers NV. Current insights into renal ciliopathies: what can genetics teach us? Pediatric Nephrology. 2013; 28(6):863–874. [PubMed: 22829176]

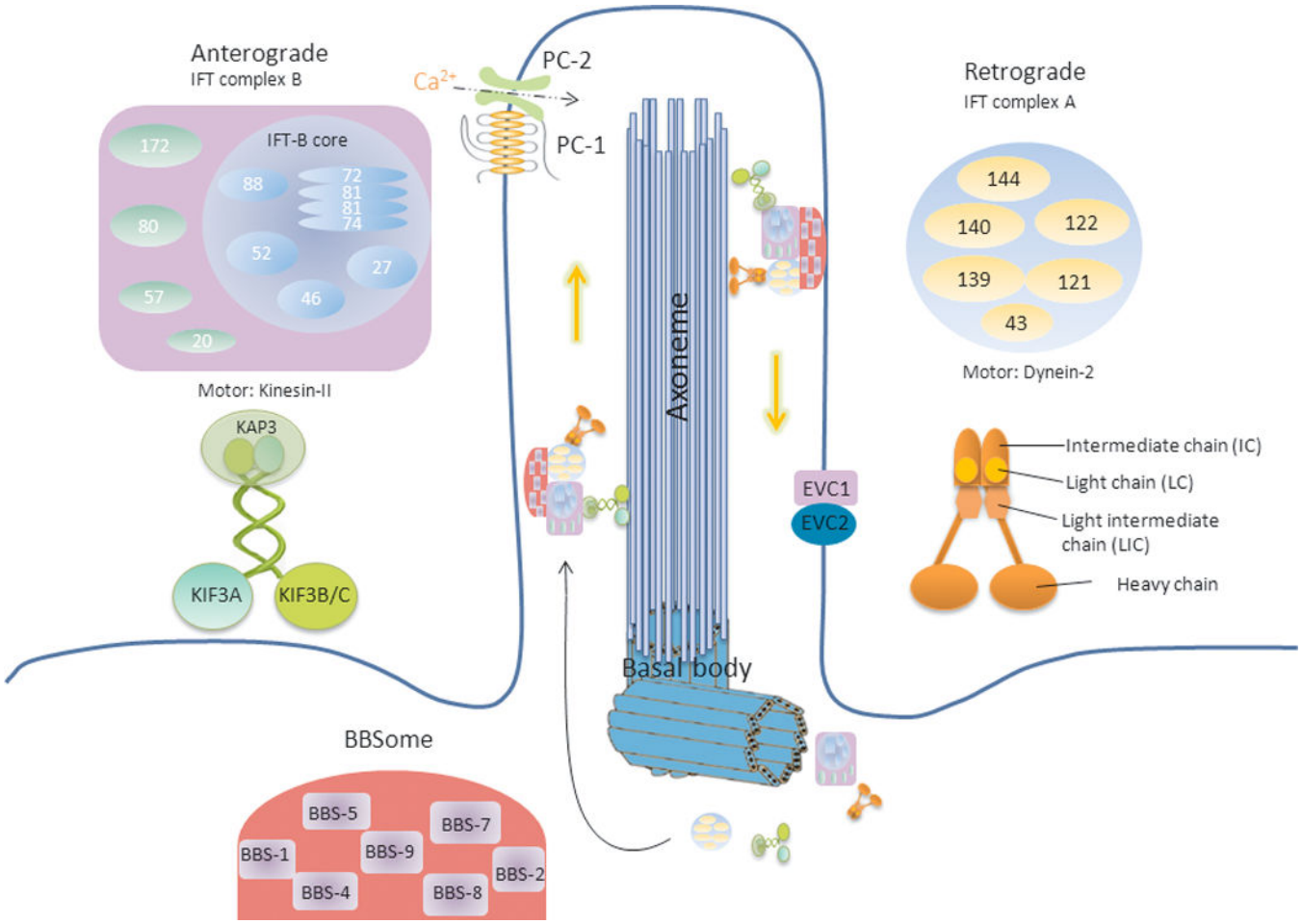

Figure 1.

The primary cilium and ciliary proteins (adapted from (28, 87, 234, 235)). The structure of primary cilia is conserved throughout evolution with a basal body (“mother” centriole) and 9 peripheral MT doublets (the axoneme). The Ift-A contains 6 known proteins (Ift144, Ift140, Ift139, Ift122, Ift121 and Ift43) and in charge of retrograde transport (from ciliary tip back to the cell body) with cytoplasmic dynein-2 as motor. Ift-B contains 14 known proteins (Ift20, Ift22, Ift25, Ift27, Ift46, Ift52, Ift54, Ift57, Ift70, Ift74/Ift72, Ift80, Ift81, Ift88 and Ift172) and is involved in anterograde transport (from the base to ciliary tip) with heterotrimeric kinesin-II as motor. Ift81 and Ift74/72 form a tetrameric complex and interact with Ift88, Ift52, Ift46 and Ift27 formed the core of complex B. Besides Ift motors and Ift complexes, BBS proteins are also important for cilia formation and maintenance. Seven highly conserved BBS proteins (BBS1, BBS2, BBS4, BBS5, BBS7, BBS8 and BBS9) formed BBSome. Evc and Evc-2 are located at the basal body and the base of the axoneme. Other proteins like OFD, NEK, Nephrocystins and MKS proteins are found localized in the basal body. And mutation of these proteins caused diseases.

Table 1

Currently known genes that are involved in skeletal ciliopathies

Disease	Ift complex A	Ift complexes B	Ift Motors	others	References
JATD	*TTC21B, WDR19, Ift140*	*Ift80*	*DYNC2H1*		(35, 108, 109, 111, 233)
MSS	*Ift140*				(111)
BBS				*BBS1-BBS16*	(114)
EVC				*Evc and Evc2*	(117–120)
WAD				*Evc2*	(121)
OFD				*OFD1*	(126)
SRP type II			*DYNC2H1*	*NEK1*	(128, 131)
SRP type III		*Ift80*	*DYNC2H1*		(35, 130)
SRP severe type	*WDR35*				(34)
CED	*Ift122, Ift43, WDR35, WDR19*				(109, 132, 135–137)
MKS				*BBS2, BBS4, BBS6, MKS1/FLJ20345, MKS3/TMEM67, TMEM216, CEP290, RPGRIP1L, CC2D2A, TCTN2, B9D1, B9D2, and NPHP3*	(114)

Jeune asphyxiating thoracic dystrophy (JATD), Intraflagellar transport (Ift), Mainzer-Saldino-syndrome (MSS), Bardet-Biedl syndrome (BBS), Ellis-van Creveld syndrome (EVC), WAD (Weyers acrofacial dysostosis), oralfacialdigital syndrome (OFD), short rib polydactyly syndromes (SRP), cranioectodermal dysplasia (CED), Meckel syndrome (MKS)

Front Biosci (Landmark Ed). Author manuscript; available in PMC 2015 March 19.

Table 2

Current mouse models to study the function of Ift-A proteins in bone development

Gene	Mouse models	Mutation	Cilia	Phenotype	Pathways	Ref
Ift139	Ift139^{alien}	ENU mutagenesis, complete loss-of-function	Short and bulb-like structure cilia with accumulation of complex B proteins in the cilia tip	Defects in limbs, eyes, skull and brain development.	Overactivated Shh pathway Ift139 is the negative regulator in the Shh pathway downstream of Smo and upstream of Gli2, no significant change in Wnt pathway.	(95, 96)
Ift122	Ift122- null	Exon 1–3 mutation of *MED1*, null mutation	Cilia loss in the homozygous and malformed cilia in heterozygous	Usually die between E10.5 to E13.5. Exencephaly, delay in limb development, defects of the ventral portion of the head, rostral neural tube, eye and branchial arches.	Impaired Shh due to reduced Gli2/Gli3 and Gli3 repressor functions.	(97)
	Ift122^{sopb}	ENU- mutagenesis, complete loss-of-function	Short and swollen cilia with complex B proteins accumulation	Die around E13.5. Neural defects, pre-axial polydactyly, enlarged bronchial arches, and ocular defects.	Enhanced Shh with Gli2 and Gli3 accumulation in the cilia tips but absent of TULP3 in cilia.	(158)
Ift144	Ift144^{twt}	ENU- mutagenesis, partial loss-of-function	Relatively normal cilia structure but reduced frequency	Die at E11.0. Polydactyly, small rib cages, cleft palate and severe craniofacial anomalies.	Ift144^{twt} MEFs respond weakly to stimulation with upstream Hh agonists, a general increase or ectopic activation of Hh in Ift144^{twt} embryos, particularly in the facial prominences and limbs.	(160)
	Ift144^{dmhd}	ENU- mutagenesis complete loss-of-function	Short and had highly disrupted axoneme	Die after E13.0. Polydactyly and craniofacial abnormalities. Smaller forelimb paddle, with truncation in the PD and to a lesser extent the AP axes.	Less activation of the Shh pathway in the caudal neural tube.	(160, 161)
	Ift144^{twt}Ift122^{sopb}	Double mutation	Similar to Ift144^{dmhd}	Similar to Ift144^{dmhd}.	Less Shh pathway activity.	(161)
	Ift144^{twt}Dync2h1^{mmi}	Double mutation	Reduced cilia number, cilia swollen in Dync2h1^{mmi}	Partially rescued most ventral neural cell type, and the floor plate.	Partial rescue of Shh signaling.	(161)
WDR35 (Ift121)	WDR35^{yet}	ENU- mutagenesis, complete loss-of-function	Cilia loss with Ift88 accumulated in the basal body	Usually die at E12.5. Severe defects in cardiovascular, embryo turning, and limb outgrowth and patterning. Failure of the somite derivatives.	Not reported	(34)
	WDR^{tm2a}	“targeted trap” null allele	Not reported	Phenocopies WDR35^{yet}.	Not reported	(34)
Ift140	Ift140^{null}	Germline deletion with C57Bl/6 Prm-Cre	Not reported	Die at mid-gestation.	Not reported	(162)
	Ift140^{cauli}	ENU- mutagenesis, “possibly damaging” mutation	Cilia morphology was severely disrupted with broader and bulbous appearance	Start to die at E13.5. Exencephaly, anophthalmia, severely disorganised ribs with extensive exostoses, vertebral and palatal defects, agenesis/	Ectopic Hh signaling activation and reduced Gli3 repressor production.	(163, 164)

Gene	Mouse models	Mutation	Cilia	Phenotype	Pathways	Ref
				hypoplasia of the craniofacial skeleton, and polydactyly of the hindlimbs. hypoplasia of the craniofacial skeleton, and polydactyly of the hindlimbs.		
	Ift140$^{-/-}$	Germline deletion with CMV-Cre	Not reported	Similar to Ift140^{cauli}.	Not reported	(164)

Table 3

Current mouse models to study the function of Ift-B proteins in bone development

Gene	Mouse models	Mutation	Cilia	Phenotype	Pathways	Ref
Ift80	$Ift80^{gt/gt}$	Gene trap, hypomorph with low level wild-type transcript production	Normal cilia	Usually die perinatally. Severe growth retardation with short long bones, narrow ribcage and polydactyly	Less Hh activity.	(70)
Ift88	$Ift88^{Tg737Rpw}$ (ORPK)	Transgene insertion-induced hypomorphic allele	Stunted and malformed cilia	Survive to young adulthood. Scruffy fur, severe growth retardation, cystic renal phenotype, preaxial polydactyly, defects in skeletal patterning and growth with craniofacial abnormalities, cleft palate, unfused tibia and fibula, and significantly smaller growth plates.	Defects in PDGFR-α/PDGF-A signaling.	(168–171)
	$Ift88^{\Delta 2-3\beta Gal}$ ($Ift88^{tm1Rpw}$)	A Null mutation	Cilia loss	Arrested at mid-gestation with neural tube defects, enlargement of the pericardial sac and left-right asymmetry defects.	Reduced expression of *Shh* and *Hnf3β* in midline. No changes in *Shh* or its downstream genes in limb bud.	(91, 170)
	$Ift88^{fxo}$ ($Ift88^{hypo}$)	ENU- mutagenesis, null mutation	Lack nodal cilia	Dies at E12.5. Sharp angle of the mesencephalic flexure, abnormal brain morphology and preaxial polydactyly.	Disrupted Hh signaling with loss of both Gli activator function and Gli repressor function in the limbs.	(56, 173)
	$Ift80^{flox/flox}$; Prx1-Cre	Deletion in limb mesenchyme	Cilia loss	Severe polydactyly and defects in endochondral bone formation.	Aberrant Shh and Ihh signaling.	(174)
	$Ift80^{flox/flox}$; Msx2-Cre	Deletion in limb ectoderm	Cilia loss	No overt effect on limb patterning.	Not reported.	(174)
	$Ift80^{flox/flox}$; Col2α-Cre	Deletion in committed chondrocyte	Cilia loss	Postnatal dwarfism and premature loss of the growth plate with down-regulated proliferation and up-regulated hypertrophic differentiation of the chondrocytes. Thicker	Reduced Hh but elevated Wnt/β-catenin (reduced Sfrp5) signaling. Uprelated Hh signaling in articular cartilage with reduced Gli3 repressor/ Gli3 activator.	(93) (176) (175)

Gene	Mouse models	Mutation	Cilia	Phenotype	Pathways	Ref
				articular cartilage with increased cell density and OA symptoms. articular cartilage with increased cell density and OA symptoms. articular cartilage with increased cell density and OA symptoms.		
Ift172	Ift172^{wim}	ENU- mutagenesis, a null mutation	Lack nodal cilia	Arrested at E10.5–11.5. Open neural tube in the head that lacked the normal groove on the ventral midline.	Strong defect in Shh signaling. Normal Wnt signaling.	(56) (178)
	Ift172^{avc1}	ENU- mutagenesis, partial loss of function	Defects in cilia	Die at birth. Anomalies in vertebral, trancheoesophageal and limb, defects in cardiac, anal atresia, renal dysplasia and hydrocephalous.	Defects in Hh signaling with reduced Gli3 processing and Gli2 accumulation.	(92)
	Ift172^{Slb}	Conventional knockout, a null mutation	Short and without visible microtubules	Die between E12.5 and 13.0. Severe craniofacial malformations, defects in brain patterning, failure to close the neural tube and exencephaly.	*Shh* and *Gli1* decreased in the developing forebrain and midbrain.	(179)
	Ift172$^{\Delta/\Delta}$	CMV-Cre–mediated germline deletion	Not reported	Embryonic lethality. Neural tube defects (Similar to Ift172^{wim} and 172^{Slb})	Not reported	(180)
	Ift172$^{f/t}$; Prx1-Cre	One allele is germline deletion and another is only deleted in the developing limb bud mesenchyme	Not reported	Eight digits on each forelimb and a single extra digit on each hind limb.	Not reported	(180)
Ift20	Ift20^{Flox}; Prm-Cre	Germline deletion	Not reported	Die before birth	Not reported	(183)
Ift25	Ift25^{neo} and Ift25^{null1}	Null mutation	Normal cilia	Die at birth. Omphaloceles, polydactyly with a preaxial digit duplication, micrognathia, cleft palate and malalignment of the sternal vertevbrae.	Ciliary accumulation of Shh components and attenuated Shh.	(185)
Ngd5 (Ift52)	Ift52^{hypo}	Partial loss-of-function mutations	Not reported	Tight mesencephalic flexure, left-right and ventral midline defects, polydactyly and craniofacial defect.	Defects in Hh pathway in limb buds.	(173)
Traf3ip1/MIP-T3 (Ift54)	Traf3ip1^{GT}	Gene Trap	Cilia disrupt	Die before E13.5.	Defects in Hh pathway.	(193)

Gene	Mouse models	Mutation	Cilia	Phenotype	Pathways	Ref
				Neural developmental defects, cardiac edema and polydactyly.	Down-regulated Shh pathway.	
				Neural developmental defects, cardiac edema and polydactyly.	Down-regulated Shh pathway.	
				Neural developmental defects, cardiac edema and polydactyly.	Down-regulated Shh pathway.	
Hippi (Ift57)	Hippi$^{-/-}$	Conventional knockout	Defects in nodal cilia	Die predominantly prior to E10.5. Defects in left-right patterning and nervous system development.	Down-regulated Shh pathway.	(196)

Table 4

Current mouse models to study the function of Ift retrograde motors in bone development

Gene	Mouse models	Mutation	Cilia	Phenotype	Pathways	Ref
Dync2h1	Dnchc2^{lln}	ENU- mutagenesis, missense mutation	Abnormal cilia with reduced length and bulge along their length	Die at approximately E12.5, abnormal brain morphology, randomization of heart-looping polarity and polydactylous.	Defects in Hh pathways with high level of Smo, Gli2 and Ptch1 accumulation along the cilia with or without Shh stimulation.	(48, 204)
	Dnchc2^{GT}	Gene trap insertion, null allele	Not reported	Similar to Dnchc2^{lln}.	Not reported	(48)
	Dync2h1^{ttn}	ENU- mutagenesis, deletion in AAA domain 4	Abnormal cilia with reduced length and bulges along the axoneme	Not reported	Transportation of activated Gli2 out of cilia is blocked. Wnt signaling is normal in midgestation embryo or embryo-derived fibroblasts.	(67, 205)
	Dnchc2^{Q397Stop}	ENU- mutagenesis, null mutation	Shorter and wider cilia	Die at E12.0 or earlier with pericardial edema and heart failure. Severe defects in dorsoventral patterning of the forebrain and patterning of the spinal cord.	Both Gli activator and Gli repressor activity were significantly reduced. Disruption in Gli3 proteolytic processing and Smo localization to cilia.	(207)
	Dnchc2^{W2502R}	ENU- mutagenesis, null mutation	Shorter and wider cilia	Similar to Dnchc2^{Q397Stop}.	Similar to Dnchc2^{Q397Stop}.	(207)
	Dync2h1^{mmi}	ENU- mutagenesis, missense mutation	Swollen and filled with electron-dense particles and defects in axonemal	Defects in neural tube and motor neurons.	Not reported	(161, 206)
	Dync2h1^{lln} Ift172^{wim}	Double mutation	Absent of cilia	Similar to Ift172^{wim}.	Not reported	(204)
	Dync2h1^{lln} Ift172^{avc1} and Dync2h1$^{lln/lln}$Ift172$^{avc1/+}$	Double mutation	Normal morphology in Dync2h1$^{lln/lln}$Ift172$^{avc1/+}$	Dync2h1^{lln} phenotype can be rescued by reducing Ift172 expression, more dramatic rescue of the Dync2h1 phenotype in Dync2h1$^{lln/lln}$Ift172$^{avc1/+}$ (survived to at least E16.5 with nearly normal neural patterning in the caudal neural tube).	No Ift or Hh pathway proteins accumulate in cilia, and Hh target gene expression appears to be normal.	(204)
	Ift122^{sopb}Dync2h1^{lln}	Double mutation	Similar to Ift122^{sopb}	Similar to Ift122^{sopb}.	Ectopic activity of the Shh pathway in the neural tube. Gli2 limited to the tips of cilia and Smo was not in cilia without Shh stimulation.	(204)
	Dync2h1$^{lln/lln}$Ift122$^{sopb/+}$	Double mutation	Partially rescued the cilia morphology	Partially rescued the phenotype of Dync2h1$^{lln/lln}$ including ventral neural development.	Partially rescued Shh-dependent protein trafficking in cilia.	(204)
mD2LIC	mD2LIC$^{-/-}$	Gene targeting, null mutation	Cilia fail to form in the node	mD2LIC$^{-/-}$ died before E11.5 with defects in notochord and floorplate formation and a reduction in definitive endoderm.	Reduction in Hh activity.	(210)

Table 5

Current mouse models to study the function of Ift anterograde motors in bone development

Gene	Mouse models	Mutation	Cilia	Phenotype	Pathways	Ref
Kif3a	Kif3a-Null	Removal exon 2 in ESCs	Cilia loss	Structural abnormalities, defects in left and right asymmetry and cilia loss in embryonic node.	Not reported	(94)
	$Kif3a^{flox/flox}$; Wnt1-Cre	Deletion in neural crest lineage cells	Not reported	Die shortly after birth due to respiratory failure, severe craniofacial defects with clefting and widened frontonasal prominence.	Enhanced Hh signaling in facial mesenchyme. Impaired Hh signaling in Kif3a-deficient neural crest-derived mesenchyme.	(218, 219)
	$Kif3a^{flox/flox}$; Dermo1-Cre	Deletion in trunk and limb skeletal progenitor cells	Not reported	Die at birth, split sternum, polydactyly and defects in ribs, knee joints and limbs.	Not reported	(218)
	$Kif3a^{flox/flox}$; Prx1-Cre	Deletion in the lateral plate mesoderm	Cilia loss	Forelimb polydactyly and profound shortening of limb bones.	Disrupted Hh signaling in long bones.	(174, 218)
	$Kif3a^{flox/flox}$; Col2α1-Cre	Deletion in cartilage	Cilia disrupted (93, 220)	Postnatal dwarfism. Abnormal cranial base development and altered synchondrosis growth plate organization and function at postnatal stages.	Hh signaling significantly reduced within growth plates but enhanced and widespread all along perichondrial tissues. Chondrocytes proliferation reduced but the hypertrophic differentiation is unregulated in growth plate, Hh signaling is unchanged.	(93, 220)
	$Kif3a^{flox/flox}$; Oc-Cre	Deletion in mature osteoblast	Reduced cilia number and length	Osteopenia by 6 weeks of age and partially recovered at 16 weeks.	Impaired osteoblastic differentiation, impaired intracellular calcium response to fluid flow shear stress, and reduced Hh and Wnt response.	(221)
	Kif3a; Col3a; I 2.3-Cre	Deletion in osteoblast progenitor	Not reported	No obvious skeletal defects. Reduced bone formation in response to mechanical ulnar loading.	Not reported	(222)
Kif3b	Kif3b-Null	Null mutation with first exon replaced by neo cassette	Cilia loss	Die at mid-gestation and exhibited randomized left–right asymmetry, growth retardation, pericardial sac ballooning and neural tube disorganization.	Not reported	(225)
Kif17	$Kif17^{-/-}$(231)	Frame shift with function loss	Not reported	No gross defects	Not reported	(231)
Kif7	$Kif7^{flox/flox}$; NLS-Cre	Ubiquitous deletion with NLS-Cre	Not reported	Die at birth with severe malformations, including exencephaly, polydactyly and sternal defects.	Up-regulated full-length Gli2 while down-regulated truncated 83-kD repressor Gli3 in total embryo lysates.	(215)
	$Kif7^{maki}$	ENU- mutagenesis, Loss of function	Normal cilia	Die at the end of gestation with abnormal motor neurons and preaxial polydactyly.	Reduced processed Gli3 proteins and the ratio of processed Gli3/full-length Gli3.	(206)
	$Ift172^{wim}Kif7^{maki}$	Double mutants (206)	Disrupt cilia	Similar to $Ift172^{wim}$.	Not reported	(206)

Gene	Mouse models	Mutation	Cilia	Phenotype	Pathways	Ref
	Dync2h1^{mmi}Kif7^{maki}	Double mutants (206)	Not reported	Similar to Kif7^{maki} with greater loss of ventral neural cell types.	A stronger loss of Shh signaling than Dync2h1^{mmi}.	(206)
	Kif7-KO	Knockout allele	Normal cilia	Spinal cord defects, preaxial polydactyly, exencephaly, and microphthalmia, which mimic the Gli3 mutants phenotypes.	Reduced proteolytic processing of Gli3. Reduce Gli2 and Gli3 accumulation at the tip of cilia in response to Hh.	(216)